AD-A023 349

A WIND TUNNEL STUDY OF THE EFFECTS OF SPLITTER PLATE POSITION AND ANGLE ON THE LIFT-DRAG RATIO OF A CIRCULATION CONTROLLED ELLIPTICAL AIRFOIL

Wayne E. Rhynard, Jr.

Air Force Institute of Technology
Wright-Patterson Air Force Base, Ohio

October 1974

KEEP UP TO DATE

Between the time you ordered this report—which is only one of the hundreds of thousands in the NTIS information collection available to you—and the time you are reading this message, several *new* reports relevant to your interests probably have entered the collection.

Subscribe to the **Weekly Government Abstracts** series that will bring you summaries of new reports *as soon as they are received by NTIS* from the originators of the research. The WGA's are an NTIS weekly newsletter service covering the most recent research findings in 25 areas of industrial, technological, and sociological interest—invaluable information for executives and professionals who must keep up to date.

The executive and professional information service provided by NTIS in the **Weekly Government Abstracts** newsletters will give you thorough and comprehensive coverage of government-conducted or sponsored research activities. And you'll get this important information within two weeks of the time it's released by originating agencies.

WGA newsletters are computer produced and electronically photocomposed to slash the time gap between the release of a report and its availability. You can learn about technical innovations immediately—and use them in the most meaningful and productive ways possible for your organization. Please request NTIS-PR-205/PCW for more information.

The weekly newsletter series will keep you current. But *learn what you have missed in the past* by ordering a computer **NTISearch** of all the research reports in your area of interest, dating as far back as 1964, if you wish. Please request NTIS-PR-186/PCN for more information.

WRITE: Managing Editor
5285 Port Royal Road
Springfield, VA 22161

Keep Up To Date With SRIM

SRIM (Selected Research in Microfiche) provides you with regular, automatic distribution of the complete texts of NTIS research reports *only* in the subject areas you select. SRIM covers almost all Government research reports by subject area and/or the originating Federal or local government agency. You may subscribe by any category or subcategory of our WGA **(Weekly Government Abstracts)** or **Government Reports Announcements and Index** categories, or to the reports issued by a particular agency such as the Department of Defense, Federal Energy Administration, or Environmental Protection Agency. Other options that will give you greater selectivity are available on request.

The cost of SRIM service is only 45¢ domestic (60¢ foreign) for each complete microfiched report. Your SRIM service begins as soon as your order is received and processed and you will receive biweekly shipments thereafter. If you wish, your service will be backdated to furnish you microfiche of reports issued earlier.

Because of contractual arrangements with several Special Technology Groups, not all NTIS reports are distributed in the SRIM program. You will receive a notice in your microfiche shipments identifying the exceptionally priced reports not available through SRIM.

A deposit account with NTIS is required before this service can be initiated. If you have specific questions concerning this service, please call (703) 451-1558, or write NTIS, attention SRIM Product Manager.

This information product distributed by

NTIS U.S. DEPARTMENT OF COMMERCE
National Technical Information Service
5285 Port Royal Road
Springfield, Virginia 22161

UNCLASSIFIED

SECURITY CLASSIFICATION OF THIS PAGE (When Data Entered)

REPORT DOCUMENTATION PAGE		READ INSTRUCTIONS BEFORE COMPLETING FORM
1. REPORT NUMBER GAE/AE/74D-22	2. GOVT ACCESSION NO.	3. RECIPIENT'S CATALOG NUMBER AD-A023349
4. TITLE (and Subtitle) A WIND TUNNEL STUDY OF THE EFFECTS OF SPLITTER PLATE POSITION AND ANGLE ON THE LIFT-DRAG RATIO OF A CIRCULATION CONTROLLED ELLIPTICAL AIRFOIL		5. TYPE OF REPORT & PERIOD COVERED MS Thesis 6. PERFORMING ORG. REPORT NUMBER
7. AUTHOR(s) Wayne E. Rhynard Jr. Captain USAF		8. CONTRACT OR GRANT NUMBER(s)
9. PERFORMING ORGANIZATION NAME AND ADDRESS Air Force Institute of Technology (AFIT/EN) Wright-Patterson AFB, Ohio 45433		10. PROGRAM ELEMENT, PROJECT, TASK AREA & WORK UNIT NUMBERS
11. CONTROLLING OFFICE NAME AND ADDRESS Aeronautical Systems Division (ASD/XRHD) Wright-Patterson AFB, Ohio 45433		12. REPORT DATE October 1974 13. NUMBER OF PAGES 80
14. MONITORING AGENCY NAME & ADDRESS (if different from Controlling Office)		15. SECURITY CLASS. (of this report) Unclassified 15a. DECLASSIFICATION/DOWNGRADING SCHEDULE

16. DISTRIBUTION STATEMENT (of this Report)

Approved for public release; distribution unlimited.

17. DISTRIBUTION STATEMENT (of the abstract entered in Block 20, if different from Report)

PRICES SUBJECT TO CHANGE

18. SUPPLEMENTARY NOTES

Approved for public release; IAW AFR 190-17
Jerry C. Hix, Captain, USAF
Director of Information

19. KEY WORDS (Continue on reverse side if necessary and identify by block number)

Airfoil Testing
Boundary Layer Control
Blowing
Circulation Control
Splitter Plate

20. ABSTRACT (Continue on reverse side if necessary and identify by block number)

Wind tunnel tests were conducted to determine the effects of splitter plate position and angle on the lift-to-drag ratio of a circulation controlled airfoil. The model was a 20 percent thick, five percent cambered elliptical airfoil, with a blowing slot for circulation control located at the 96 percent chord position on the upper surface. A splitter plate of 1.5-in. chord was mounted

(see Reverse Side)

DD FORM 1 JAN 73 1473 EDITION OF 1 NOV 65 IS OBSOLETE

UNCLASSIFIED

SECURITY CLASSIFICATION OF THIS PAGE (When Data Entered)

Block #20

on the lower aft surface of the airfoil in five different test configurations. The tests were run at a constant Reynolds number, based on the model chord, of 7.7×10^5, while the angle of attack and the secondary blowing were varied at each test increment.

It was found that when moderate blowing was applied, the splitter plate caused increases in the section lift coefficient of as much as 99 percent over the values attained on the model without a splitter plate. It was further found that above certain blowing levels, some of the splitter plate configurations resulted in a reduction in the section total drag coefficient of as much as 25 percent below that of the airfoil without a splitter plate. The lift-to-drag ratio increased steadily as the splitter plate was moved aft and as its angle was adjusted toward 45 degrees. The maximum lift-to-drag ratio obtained was 100 percent higher than that attained at the same blowing level without the splitter plate.

1 a

A WIND TUNNEL STUDY OF THE EFFECTS OF SPLITTER PLATE POSITION AND ANGLE ON THE LIFT-DRAG RATIO OF A CIRCULATION CONTROLLED ELLIPTICAL AIRFOIL

THESIS

GAE/AE/74D-22 Wayne E. Rhynard Jr.
Captain USAF

Approved for public release; distribution unlimited.

A WIND TUNNEL STUDY OF THE EFFECTS OF SPLITTER PLATE POSITION AND ANGLE ON THE LIFT-DRAG RATIO OF A CIRCULATION CONTROLLED ELLIPTICAL AIRFOIL

THESIS

Presented to the Faculty of the School of Engineering
of the Air Force Institute of Technology

Air University

in Partial Fulfillment of the
Requirements for the Degree of

Master of Science

by

Wayne E. Rhynard Jr., B.S.
Captain USAF

Graduate Aeronautical Engineering

October 1974

Preface

This study investigated the effects of splitter plate position and angle on the lift-to-total drag ratio of a cambered, circulation controlled, elliptical airfoil. It is hoped that the results will be of value to future investigations of high-lift devices.

I wish to express my appreciation to Dr. Milton E. Franke, my advisor, Professor Harold C. Larsen, and Mr. James Snyder, ASD/XRHD, for their counsel throughout the project. In addition, Mr. Millard Wolfe and the AFIT workshop staff deserve many thanks for their timely and effective airfoil modifications. Special thanks go to Mr. Wales S. Whitt for his invaluable assistance during wind tunnel set-up and testing.

Further gratitude is expressed to Mr. Julius Becsey, ARL, who wrote the data reduction computer programs and made his equipment available for the data reduction process. Thanks also go to Mr. Henry Maurer of Tech Photo, for his excellent photographic support, and my very sincere appreciation is extended to Capt Thomas A. Stevenson for his advice and consultation throughout the study. Finally, many thanks go to my wife, [redacted] for her patience and support throughout this endeavor.

Wayne E. Rhynard Jr.

Contents

List of Figures

List of Tables

List of Symbols

α_g	Geometric angle of attack, degrees
β	Splitter plate deflection from model chord line, degrees
c	Model chord length, ft
C_p	Pressure coefficient, $(p-p_o)/q_o$
C_{p_ℓ}	Pressure coefficient on the lower surface of the airfoil
C_{p_u}	Pressure coefficient on the upper surface of the airfoil
C_{d_o}	Section profile drag coefficient, (see Section IV)
C_{d_t}	Section total drag coefficient, $C_{d_o} + C_\mu$
C_ℓ	Section lift coefficient, $C_n \cos\alpha_g$
C_n	Section normal force coefficient, $N/q_o c$
C_μ	Momentum coefficient, $\dot{m}V_j/q_o c$
ℓ/d	Section lift-to-total drag ratio
$\dot{m}$	Mass flow rate of blowing air per unit span, lbm/sec
N	Normal force per unit span, lb_f
p	Local static pressure, psfg
p_o	Free stream static pressure, psfg
q	Local dynamic pressure, psfg
q_o	Free stream dynamic pressure, psfg
Re	Reynolds number, based on c
V_j	Velocity at the slot, ft/sec
V_o	Free stream velocity, ft/sec

Abstract

Wind tunnel tests were conducted to determine the effects of splitter plate position and angle on the lift-to-drag ratio of a circulation controlled airfoil. The model was a 20 percent thick, five percent cambered elliptical airfoil, with a blowing slot for circulation control located at the 96 percent chord position on the upper surface. A splitter plate of 1.5-in. chord was mounted on the lower aft surface of the airfoil in five different test configurations. The tests were run at a constant Reynolds number, based on the model chord, of 7.7×10^5, while the angle of attack and the secondary blowing were varied at each test increment.

It was found that when moderate blowing was applied, the splitter plate caused increases in the section lift coefficient of as much as 99 percent over the values attained on the model without a splitter plate. It was further found that above certain blowing levels, some of the splitter plate configurations resulted in a reduction in the section total drag coefficient of as much as 25 percent below that of the airfoil without a splitter plate. The lift-to-drag ratio increased steadily as the splitter plate was moved aft and as its angle was adjusted toward 45 degrees. The maximum lift-to-drag ratio obtained was 100 percent higher than that attained at the same blowing level without the splitter plate.

I. Introduction

In recent years, considerable attention has been concentrated on the subject of low-speed, high-lift flight. This area is of great importance to present and future aviation because of its application to the development of vertical and short field take off and landing, as well as to the attainment of increased endurance and reduced turn radius.

One means of obtaining high lift at low speed is through airfoil circulation control, which may be described as the process of delaying flow separation from an airfoil by re-energizing the boundary layer. This is accomplished by blowing relatively high speed air over the rear upper surface of the airfoil. On airfoils with blunt trailing edges, the Coanda effect keeps the air attached as it moves around the trailing edge, transferring the front and rear stagnation points to the lower surface. In addition to increasing the section lift coefficient, C_ℓ, circulation control results in a decrease in the section profile drag coefficient, C_{d_o}.

Previous Studies

Using the uncambered circulation control airfoil shown in Fig. 1, Kind and Maull obtained C_ℓ's as high as 3.3 (Ref 5:176). Williams (Ref 14), Walters (Ref 13), and

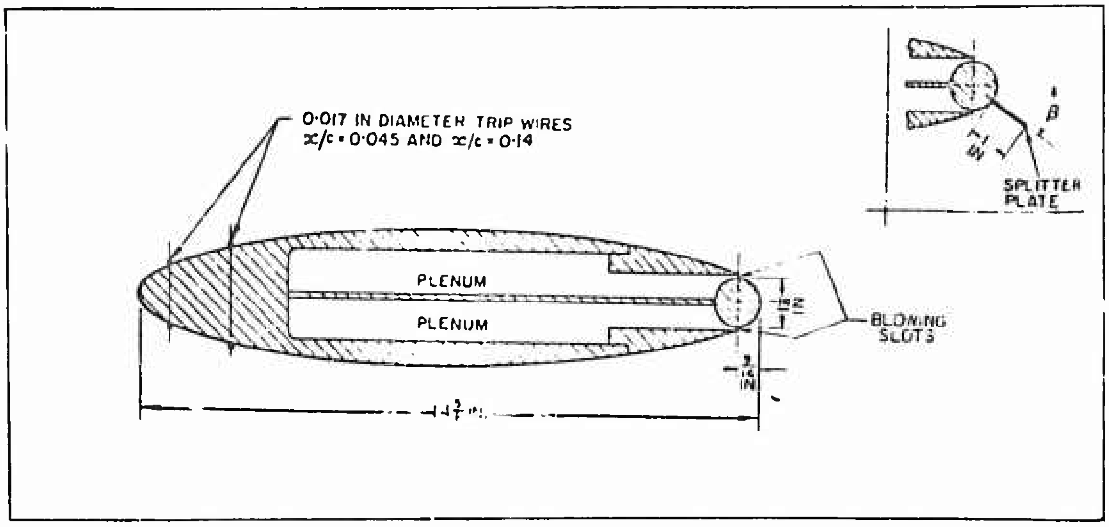

Fig. 1. Cross Section of the Kind and Maull Airfoil (Ref 5:172)

Englar (Ref 3), in further tests with circulation control airfoils, obtained even higher C_ℓ values. In addition, Kind and Maull found that by attaching a flat metal plate, which they called a splitter plate, with a one inch chord and a span equal to that of the model, the lift-to-drag ratio, ℓ/d, could be increased from 30 to 42 (Ref 5:180). Attached to the lower surface of the trailing edge at a 45 degree angle to the model chord line, the plate reduced the mixing losses, and therefore, the drag. Although Kind and Maull experimented but briefly with the splitter plate, they speculated that an optimum splitter plate angle probably exists for a given airfoil (Ref 5:179-181).

In contrast to Kind and Maull's uncambered, elliptical airfoil, Stevenson used an airfoil that combined 5 percent camber with a 20 percent thick elliptical cross section. This airfoil is shown in Fig. 2. It was found to achieve a maximum ℓ/d of 56 when fitted with a splitter plate of 1.5-in. chord. The plate was fixed at 45 degrees to the model chord line at the 99 percent chord position on the lower surface (Ref 12:71). Though the model attained higher ℓ/d values than were achieved by Kind and Maull's uncambered model, Stevenson recommended that further study be applied to determining the optimum splitter plate position and angle for maximum ℓ/d, and that the amount of secondary blowing be increased beyond that applied in his tests (Ref 12:31,32).

Objective

The purpose of the current study was to modify the airfoil used by Stevenson and determine the splitter plate position and angle for maximum ℓ/d. Tests were run in the Air Force Institute of Technology (AFIT) Five-Foot Wind Tunnel at five different blowing rates, six splitter plate configurations, and throughout a 12 degree range of geometric angles of attack.

II. Description of Apparatus

Wind Tunnel

The wind tunnel tests were conducted in the AFIT Five-Foot Wind Tunnel. It is an open circuit, closed test section wind tunnel with a maximum speed of 350 miles per hour empty. A two-dimensional test section was simulated by the installation of 2 large wooden side boards, making the tunnel cross section 60 in. by 30 in. The two-dimensionality was further increased by the attachment of large circular, bevelled endplates 0.19-in. thick to each end of the airfoil for the purpose of stripping the boundary layer. Secondary air for circulation control blowing was tapped from the Jet Propulsion Laboratory compressed air supply.

Airfoil

The experimental airfoil, shown in Figs. 3 and 4, was a 20 percent thick, five percent cambered ellipse, symmetrical about the front and rear. The span of the model was 2.17 ft, while the chord was 1.67 ft. It was equipped with 48 static pressure taps distributed on the upper and lower surfaces.

Blowing air was routed through an annealed copper pipe to the fiber glass plenum chamber. The chamber, which had a diverging-converging cross section, extended the entire

span of the model. A 0.02-in. wide blowing slot at the minimum area of the converging portion of the chamber allowed the blowing air to flow along the upper, rear airfoil surface at the 96 percent chord position. Further details of the basic model design are available in Stevenson's report (Ref 12:9-11).

Airfoil Modifications

As a result of the static pressure tap spacing along the lower surface of the airfoil, it was feasible to mount the splitter plate in two different positions. These were the 95.3 and 99 percent chord positions on the lower surface. The model was modified, as shown in Figs. 3 and 4, by grooving two, 0.06-in. radius, semi-circular, spanwise notches into the lower surface of the airfoil at these two locations. The notches served as receptacles for the leading edge of the splitter plate, allowing smooth rotation of the plate when its angle was adjusted. When not in use, one or both of the notches were filled with modeling clay and smoothed to prevent flow disruption. In the remaining discussion, the 95.3 percent chord location will be referred to as forward, and the 99 percent position as aft.

The splitter plate had a 1.5-in. chord, a maximum thickness of 0.13 in., and was tapered to a sharp trailing edge. It was fitted with endplates containing one hole each, which, when aligned with small holes in the model

endplates and pinned, allowed the plate to be set at β's, or angles with the model chord line, of 45 and 60 degrees in the forward location and 30, 45 and 60 degrees when located aft. Finally, the leading edge of the splitter plate was rounded to enable smooth adjustment when lodged in the semi-circular notches on the lower airfoil surface.

Pitot Tube Apparatus

The purpose of the pitot tube apparatus was to determine the uniformity of spanwise total pressure along the blowing slot. The apparatus, which is shown in Fig. 5, consisted of a two inch long tube with a 0.02-in. diameter that was mounted on a metal slide which could be moved along the entire 2.17-ft span of the airfoil. This allowed the tube to point directly into the blowing slot as each pressure reading was recorded along the span.

Flowmeter

A 0.5-in. throat diameter venturi tube was used to measure the mass flow rate of the blowing air. It was calibrated against a 0.5-in. National Bureau of Standards venturi to an accuracy of ±0.5 percent. Pressure readings were taken from flange taps at the throat and upstream of the throat, while the temperature was obtained from a copper-constantan thermocouple located just upstream of the venturi.

Wake Survey Rake

A total head wake survey rake was designed and constructed to measure the momentum deficit of the airfoil wake. The rake was equipped with 96 total head tubes and two static tubes, all of 0.0625-in. outside diameter and spaced 0.25 in. apart. The rake, shown in Fig. 6, was adjustable from the tunnel floor boundary layer to 10 in. above mid-tunnel. The airfoil section of the rake spanned the tunnel from top to bottom and was situated 37 in., or 1.85 chord lengths, behind the airfoil.

Manometers

A 100-tube bank of red oil manometers was connected to the wake survey rake. A total of 98 of the tubes were utilized, and the bank was inclined at 60 degrees to the vertical so that changes on the rake could be read more accurately. In addition, 50 tubes of a 100-tube bank of alcohol manometers were used to measure the static pressure on the airfoil and the dynamic pressure of the free stream and test section. Finally, two 60-in. manometers were used on the venturi pressure taps, and an 8-in. U-tube plus two 30-in. manometers were used to measure the total pressure in the plenum chamber.

III. Experimental Procedures

After leak tests were conducted on the blowing system, all model and wind tunnel components were checked for proper operation. The actual test sequence began with the establishment of the airfoil configuration by setting a specific splitter plate position and angle. The blowing rate was then established by setting predetermined venturi pressures. Next, the tunnel speed was brought to 76 feet per second, after which the geometric angle of attack was varied from -6 to +6 degrees. The angle of attack sequence began at 0 degrees and proceeded in order to -6, -4, -2, 0, +2, +4, +6, and 0 degrees. At each angle of attack increment, the manometer banks were photographed and the plenum chamber total pressure and venturi data recorded. After the angle of attack sequence was completed, the blowing rate was changed and the sequence repeated until each of the five blowing rates had been tested. Then, the entire procedure was repeated for a different airfoil configuration. In addition, 20 percent of the record runs were repeated as a check for accuracy, while periodic surveys were conducted of the total pressure uniformity along the blowing slot.

IV. Data Reduction

Section Lift Coefficient

C_ℓ was calculated according to the equation

$$C_\ell = C_n \cos \alpha_g \tag{1}$$

where C_n is the section normal force coefficient and α_g is the geometric angle of attack (Ref 9:169). C_n was calculated by numerical integration of the pressure coefficients around the airfoil. The integration was performed by the trapezoidal rule on the Hewlett-Packard 9100A Calculator and 9107A Digitizer, according to the equation

$$C_n = \int_0^1 (C_{p_\ell} - C_{p_u}) d(\tfrac{x}{c}) \tag{2}$$

where C_{p_ℓ} and C_{p_u} are the pressure coefficients on the lower and upper surfaces respectively, and $\frac{x}{c}$ is distance along the chord line (Ref 13:16).

Momentum Coefficient

The momentum or blowing coefficient, C_μ, is a measure of the amount of blowing applied to a circulation control airfoil. It was computed as shown in Eq (3).

$$C_\mu = \frac{\dot{m} V_j}{q_o c} \tag{3}$$

where $\dot{m}$ is the mass flow rate of the blowing per unit span, V_j is the blowing velocity at the slot, q_o is the free stream dynamic pressure, and c is the chord (Ref 7:195).

Section Total Drag Coefficient

The section profile drag coefficient, C_{d_o}, and the section total drag coefficient, C_{d_t}, were calculated using Eqs (4) and (5) given by Englar (Ref 3) and Kind and Maull (Ref 5), respectively.

$$C_{d_o} = \frac{2}{c}\int_0^h \left(\sqrt{\frac{q}{q_o}} - \frac{q}{q_o}\right) dy + \frac{\dot{m}V_o}{q_o c} \qquad (4)$$

$$C_{d_t} = C_{d_o} + C_\mu \qquad (5)$$

In these equations, q and q_o are the dynamic pressure in the wake and free stream, respectively, dy is the incremental distance between tubes on the rake, and V_o is the free stream velocity. The integral term in Eq (4) represents that portion of the section profile drag coefficient that was calculated by the momentum method of Pope (Ref 9), while the second term accounts for the fact that the blowing air flow was entirely separate from the wind tunnel air flow and did not originate upstream of the model as assumed in the momentum method (Ref 5). Again, the integration was performed according to the trapezoidal rule on the Hewlett-Packard calculator and digitizer. In Eq (5), C_μ represents the penalty paid in the production of the blowing air.

Lift-to-Drag Ratio

The ℓ/d values were computed by taking the ratio of C_ℓ to C_{d_t} as shown in Eq (6)

$$\frac{\ell}{d} = \frac{C_\ell}{C_{d_t}} \tag{6}$$

Wind Tunnel Corrections

Solid and wake blocking, along with streamline curvature corrections, were applied to C_ℓ. Solid and wake blocking corrections were also applied to C_{d_t}, V_o, q_o, and the Reynolds Number. In addition, a wake survey rake correction factor was applied to the static pressure readings of the rake.

V. Results and Discussion

General Observations

Throughout the experiment, there were noticeable quantities of oil and water present in the blowing system. While the water was merely natural condensation, the oil was the result of leaks in the Roots blowers which supplied the secondary air for blowing. The most noticeable effect of the oil was its tendency to build up along the downstream edge of the blowing slot, forming a lip, or bump, across the entire span of the model. This bump was disruptive to the flow, and in some cases resulted in loss of the Coanda effect and separation. In order to quantitatively determine the effects of the oil, several repeat runs were made, during which the airfoil was wiped free of oil before each data point was taken. The results were then compared to those of the same runs without oil removal.

It was found that the flow with oil removal generally remained attached up to angles of attack four degrees greater than achieved without removal. Also, the oil had a greater effect at C_μ's below 0.05, and these effects were independent of airfoil configuration. From -6 through +2 degrees angle of attack, C_ℓ and C_{d_t} for the two cases were indistinguishable. However, at +4 and +6 degrees angle of attack, the flow began to separate from the model with oil.

Here, the maximum difference between the coefficients for the two cases was six percent for C_ℓ and five percent for C_{d_t}. Cases where the flow was completely separated from the model without oil removal were not compared. These results indicate that the adverse effect of the oil was limited to its tendency to cause separation at slightly lower angles of attack than would have been attained with clean blowing air.

During tests at C_μ's less than 0.05, separation often occurred at +4 to +6 degrees angle of attack for all configurations. At C_μ's greater than 0.05, the tendency of the flow to separate was greatly reduced, and no separation occurred at C_μ's greater than 0.08 in the range of α_g tested. Stevenson also experienced separation at low C_μ's, and his belief that increased blowing would reduce the separation tendency was corroborated by the current study. The oil tests seemed to indicate that the presence of oil in the blowing air was the primary cause of separation at C_μ's below 0.05, while contributing factors were the physical location of the blowing slot and the small radius of curvature of the trailing edge.

A study of the photographs of the static pressure distributions around the airfoil permitted an early comparison of the flow patterns for the different configurations. For the clean configuration, it was found that the static pressure increased approximately 67 percent from the

blowing slot to the trailing edge. The pressure increases when the splitter plate was mounted in the forward position, regardless of β, was 60 percent for the same distance. However, when the splitter plate was mounted in the aft position, the increase was slightly less than 50 percent for all three plate angles. These values were relatively constant for all C_μ's and angles of attack. The percentages indicate the relative severity of the adverse pressure gradient on the model surface, and they indicate that the aft splitter plate location was most effective in reducing that gradient. Thus, the flow around the trailing edge for the aft plate location was faster, had more energy, and produced greater circulation.

Blowing Slot Pressure Survey

As shown in Table I, the total pressures measured in the first several inches of the blowing slot were as much as 20 percent lower than along the remainder of the slot. This effect was most pronounced at high C_μ's, while it was practically negligible at low blowing. The high spanwise velocity of the air as it entered the pipe at the leading edge of the plenum chamber and the geometry of the pipe-chamber combination made it impossible for the air to flow evenly into the plenum chamber. However, at lower blowing, the spanwise velocity was lower and the air was able to flow more evenly into the chamber. Since the static

pressures on the airfoil were measured at mid-span and the slot total pressure was uniform there, the test data was uneffected by the non-uniformity.

Lift Results

The lift results, shown in Figs. 7 through 12, indicate that the combination of the splitter plate and circulation control greatly increased the C_ℓ over that of the clean configuration, which attained the lowest C_ℓ's in all cases. Even without blowing, the splitter plate caused C_ℓ to increase above the clean airfoil values. The aft splitter plate position, with a β of 60 degrees, produced the highest C_ℓ at each C_μ tested, reaching a maximum value of 3.79. The aft configuration, with a β of 45 degrees, attained the second highest C_ℓ's up to a C_μ of 0.05. Above that C_μ, the two forward plate configurations achieved the second highest C_ℓ values. In all cases, the aft, 30 degree β plate configuration had the lowest C_ℓ's of all splitter plate configurations. Table II shows the configurations ranked in order of decreasing C_ℓ for $C_\mu = 0.04$ and an angle of attack of -2 degrees. It should be noted that while these relationships held for all α_g's tested, they varied somewhat as C_μ was changed. The C_μ value of 0.04 was selected because it was near the value for maximum ℓ/d. The actual C_ℓ's are given in the table, along with the percentage increase in C_ℓ over the clean airfoil value for

each listing. The results indicate that the aft splitter plate location and the steeper plate angles were most effective in achieving high C_ℓ's.

The superior C_ℓ's attained with the steeper plate angles were probably due to the fact that the jet of air from the blowing slot had a larger vertical than horizontal component as it left the airfoil at the splitter plate, resulting in the addition of the vertical thrust to the airfoil lift. The rear plate location was superior because the flow had less distance to travel against the adverse pressure gradient in moving from the blowing slot to the plate, and consequently, had more energy when it arrived at the plate.

Fig. 12 shows the variation in C_ℓ with α_g for each of the C_μ's tested. The values presented are those of the maximum lift configuration with the splitter plate at a β of 60 degrees in the aft position. The value of C_ℓ increased with both α_g and C_μ in all cases.

Drag Results

Figs. 13 through 20 present the drag results of the study. It can be seen that up to a C_μ of approximately 0.03, the clean configuration had the lowest values of C_{d_t}. However, above that C_μ the aft splitter plate positions exhibited the lowest C_{d_t} values, while the forward positions exhibited the highest values of C_{d_t} throughout the entire

range of C_μ. Table III shows the six configurations ranked in order of increasing C_{d_t} for an α_g of -2 degrees and a C_μ of 0.04. From a C_μ of 0.04 through 0.09, the aft plate location, with a β of 45 degrees, had the lowest C_{d_t} values, while the 30 and 60 degree aft plate positions gave successively higher C_{d_t} values. With the exception of the 45 degree aft minimum drag configuration, it is clear that C_{d_t} increased with forward movement and increasing angle of the splitter plate.

While C_{d_t} increased with increasing C_μ for all configurations, a study of Figs. 19 and 20 shows that the increase was due to the addition of C_μ to C_{d_o}, the section profile drag coefficient. The C_{d_o} curve in Fig. 19 demonstrates that there was a dramatic decrease in C_{d_o} as C_μ was increased. The decrease was due to the reduction in mixing losses caused by the splitter plate and to the horizontal component of the thrust created by the blowing air at the splitter plate. The thrust was most noticeable with the 30 and 45 degree aft splitter plate positions. Fig. 18 shows that the variation in C_{d_t} with α_g was quite small for each C_μ until separation approached.

Lift-to-Drag Ratio Results

The ℓ/d results are presented in Figs. 21 through 26, and Table IV lists the six configurations in order of decreasing ℓ/d for an α_g of -2 degrees and a C_μ of 0.04.

Due to the fact that it attained high C_ℓ's and the lowest C_{d_t}'s throughout most of the C_μ range tested, the aft splitter plate configuration, with a β of 45 degrees, attained the highest ℓ/d ratios for all but the very highest C_μ's. At these extreme values, the 60 degree aft position produced slightly higher ℓ/d's. Although the 60 degree aft configuration achieved the best lift results, its C_{d_t} values were much higher than those of the 45 degree aft configuration. The two forward positions and the 30 degree aft position, in that order, achieved the next highest ℓ/d values, while the clean configuration produced ℓ/d's significantly below all other values in all cases. With the exception of the 30 degree plate angle, the rear position of the splitter plate yielded the best ℓ/d results, but it is difficult to define any consistent trends for the plate angle. As a whole, all of the configurations gave their best ℓ/d results in a C_μ range of 0.03 through 0.04. A review of the drag results shows that the slope of the C_{d_t} versus C_μ curves rose rather steeply for all configurations as C_μ was increased beyond 0.04. This accounts for much of the decrease in ℓ/d values with increased blowing beyond a C_μ of 0.04.

The relative contributions of C_ℓ and C_{d_t} can be appreciated by a study of Figs. 27 through 31, which show C_ℓ versus C_{d_t} for both the clean and the aft splitter plate configurations. The steep slopes of the 45 and 60

degree splitter plate curves shows that these configurations experienced very great lift increases with relatively small increases in drag. Note that the levelling of the slope of the 45 degree curve is shown on the ℓ/d versus C_μ curves as a decrease in ℓ/d with increasing C_μ. As shown in Fig. 26, the ℓ/d varied directly with α_g for all C_μ's.

Comparison of Results With Previous Work

Figs. 32 through 37 show several results of the current study plotted with Stevenson's results for similar test conditions and configurations. The results shown are for the clean configuration and the 45 degree aft splitter plate configuration. The two C_μ's chosen from the current study were slightly higher and slightly lower than those of Stevenson, and the Reynolds Numbers were a little lower in all cases.

As shown in Fig. 32, the C_ℓ's of the clean airfoil in the current study bracketed those of Stevenson, demonstrating excellent agreement. Fig. 35 indicates that separation occurred at several points of Stevenson's test with the aft, 45 degree β configuration, causing three of his C_ℓ's to be lower than anticipated. However, his other three C_ℓ values for this configuration were in excellent agreement with those obtained in this study.

Figs. 33 and 36 show that the values of Cd_t obtained by Stevenson were somewhat lower than the values of this

study. The higher C_{d_t} values of the current study were the result of more accurate measurement of the profile drag by the wake survey rake used in this test. The rake was constructed such that the total head tubes were concentrated in the lower half of the tunnel, directly in the airfoil wake. In addition, the rake was mounted more than a full model chord length behind the airfoil, allowing the wake to reach tunnel static pressure before measurement at the rake. The lower C_{d_t} values obtained by Stevenson are reflected in his higher ℓ/d values as shown in Figs. 34 and 37.

Because of important differences in the two airfoils, the results of this study can only be qualitatively compared with those of Kind and Maull. The airfoil of Kind and Maull was symmetrical with a rounded trailing edge. There were also significant differences in the splitter plate chord and in the blowing slot thickness. Nevertheless, it was possible to compare the relative merits of some of the configurations. Kind and Maull experimented briefly with splitter plate angles of 30, 45, and 60 degrees, with the plate mounted in the vicinity of the 99 percent chord position. Though their report displayed results for an α_g of +5 degrees only, the curve shapes and relationships between configurations were exactly those of the current study as shown in Figs. 11, 17, and 31.

VI. Conclusions

A two-dimensional wind tunnel study to determine the splitter plate position and angle for maximum lift-to-drag ratio of a circulation controlled airfoil resulted in the following conclusions.

1. The section lift coefficient increases as the splitter plate position is moved aft toward the 99 percent chord location.
2. The section lift coefficient increases as the angle between the splitter plate and the airfoil chord line is increased toward 60 degrees.
3. The section profile drag coefficient and the section total drag coefficient decrease as the splitter plate location is moved aft toward the 99 percent chord position.
4. The splitter plate angle for minimum section profile drag coefficient and minimum section total drag coefficient is 45 degrees.
5. The section lift-to-total drag ratio is maximized when the splitter plate is located at the 99 percent chord position at an angle of 45 degrees to the airfoil chord line.

6. The section lift-to-total drag ratio is maximized for each splitter plate configuration when the momentum coefficient is between 0.03 and 0.04.

VII. Recommendations

It is recommended that further wind tunnel tests of circulation controlled airfoils include:

1. A determination of the contribution of pressure drag to the profile drag of the airfoil with and without a splitter plate.
2. The effects of a free-to-rotate splitter plate, able to seek its own angle with the model chord line, on the lift and drag of the airfoil.
3. A detailed flow visualization study of splitter plate effects on the airflow.

Bibliography

1. American Society of Mechanical Engineers Research Committee on Fluid Meters. Fluid Meters. New York: American Society of Mechanical Engineers, 1959.

2. Bauer, A. B. A New Family of Airfoils Based on the Jet-Flap Principle. Douglas Aircraft Company Report No. J5713. Long Beach: Douglas Aircraft Company, September 1972.

3. Englar, Robert J. Two-Dimensional Subsonic Wind Tunnel Tests of Two 15-Percent Thick Circulation Control Airfoils. NSRDC Technical Note AL-211. Bethesda: Naval Ship Research and Development Center, August 1971. AD900210.

4. Karamcheti, K. Principles of Ideal-Fluid Aerodynamics. New York: John Wiley and Sons, Inc., 1966.

5. Kind, R. J. and D. J. Maull. "An Experimental Investigation of a Low Speed Circulation-Controlled Elliptical Airfoil." The Aeronautical Quarterly, 19:170-182 (May 1968).

6. Lachmann, G. V., editor. Boundary Layer and Flow Control. Vol. I. New York: Pergamon Press, 1961.

7. McCormick, Barnes W. Jr. Aerodynamics of V/STOL Flight. New York and London: Academic Press, 1967.

8. Pankhurst, R. C. and D. W. Holder. Wind-Tunnel Technique. London: Sir Isaac Pitman and Sons, Ltd., 1952.

9. Pope, A. Wind-Tunnel Testing (Second Edition). New York: John Wiley and Sons, Inc., 1961.

10. Schlichting, H. Boundary-Layer Theory (Sixth Edition). New York: McGraw-Hill Book Co., 1968.

11. Smith, A. M. O. and J. A. Thelander. The Power Profile A New Type of Airfoil. Douglas Aircraft Company Report No. MDC J6236. Long Beach: Douglas Aircraft Company, January 1974.

12. Stevenson, Thomas A. A Wind Tunnel Study of the Lift-Drag Ratio on a Cambered Circulation Controlled Airfoil. Unpublished Thesis. Wright-Patterson Air Force Base, Ohio: Air Force Institute of Technology, June 1974.

13. Walters, R. E., et al. Circulation Control by Steady and Pulsed Blowing for a Cambered Elliptical Airfoil. NR 215-163. Morgantown: West Virginia University, July 1972. AD 751045.

14. Williams, Robert M. and H. J. Howe. Two Dimensional Subsonic Wind Tunnel Tests on a 20 Percent Thick, 5 Percent Cambered Circulation Control Airfoil. NSRDC Technical Note AL-176. Washington, D.C.: Naval Ship Research and Development Center, 1970. AD 877764.

Appendix A

Apparatus

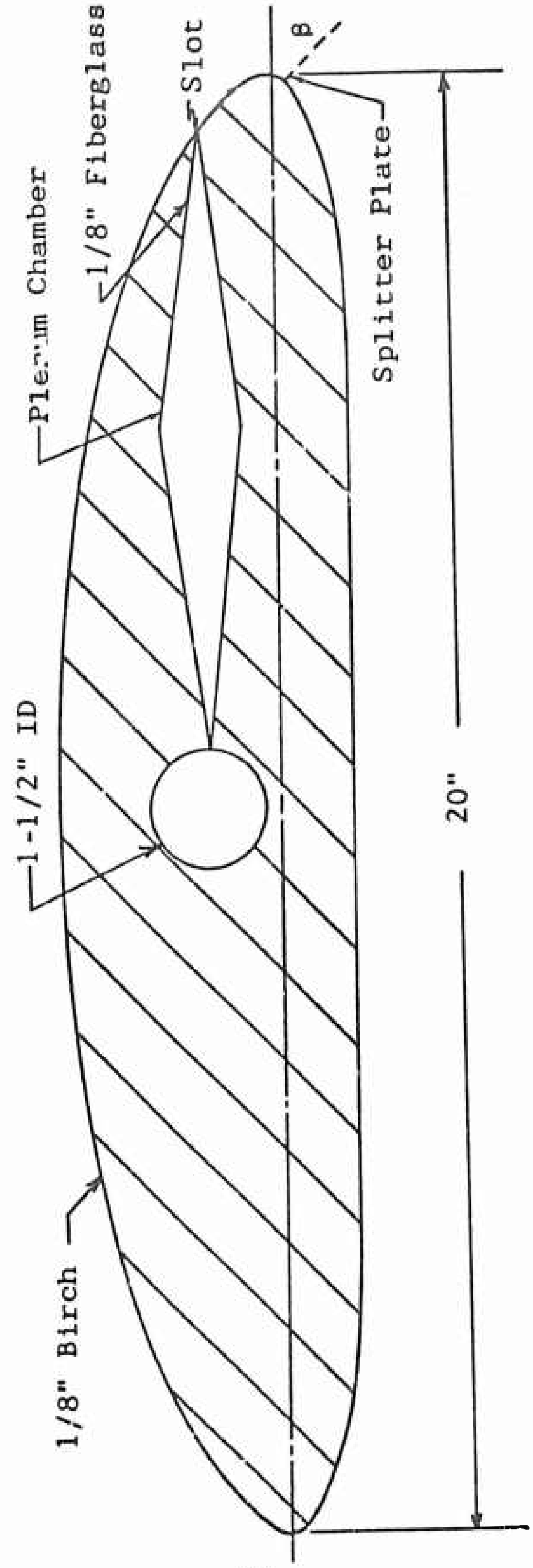

Scale: 1" = 2-1/2"

Fig. 2. Cross Section of the Stevenson Airfoil (Ref 12:45)

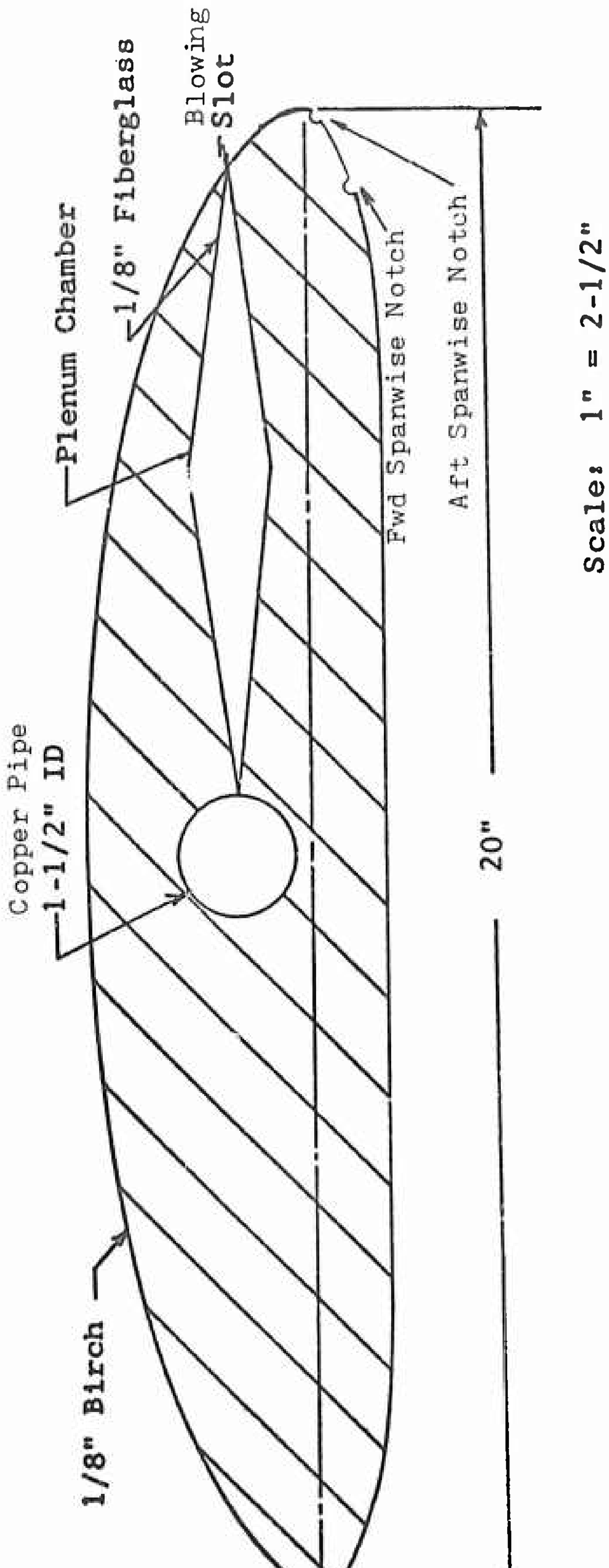

Fig. 3. Cross Section of the Modified Airfoil

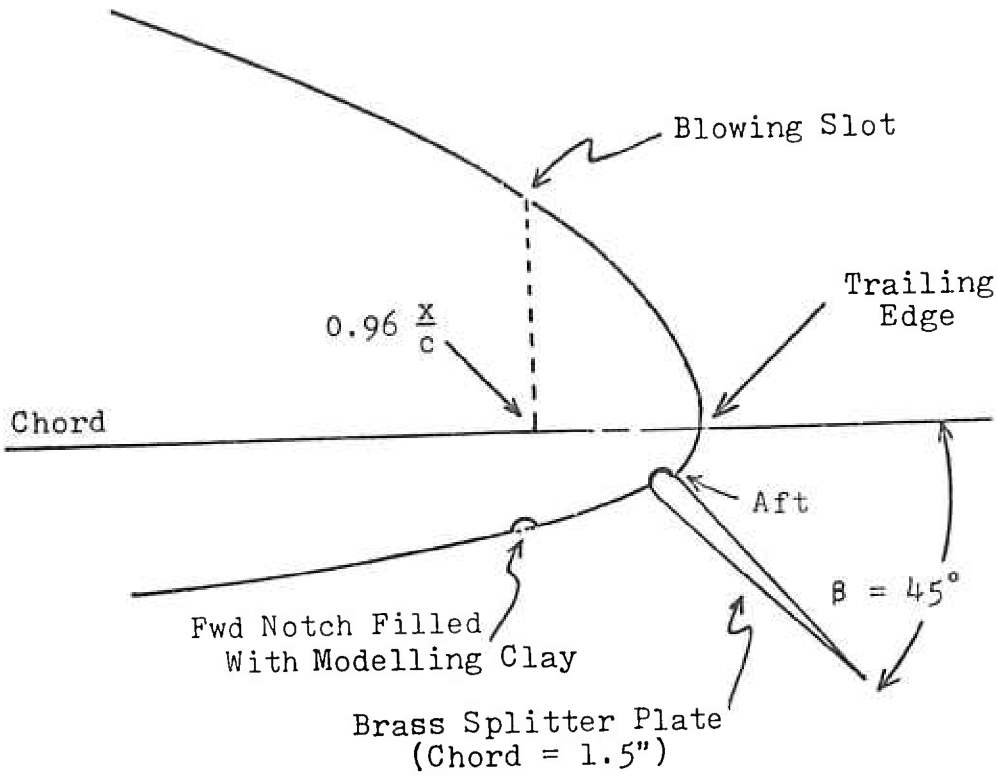

Scale: 1" = 1"

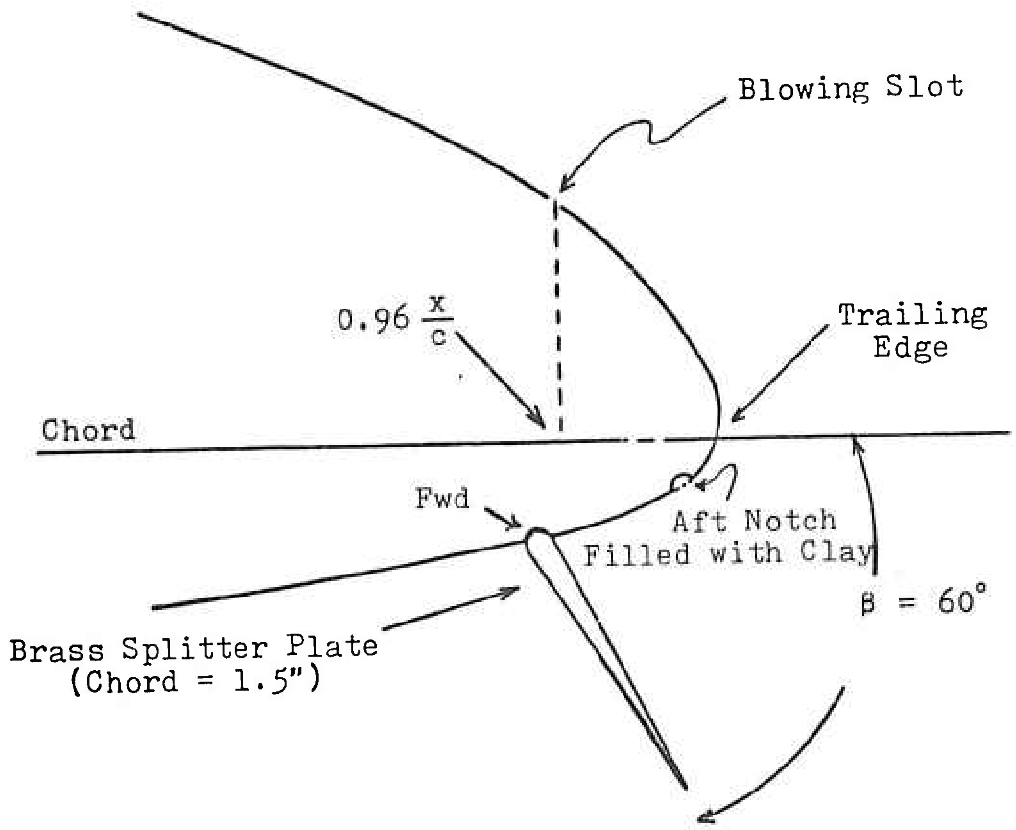

Fig. 4. Two Trailing Edge Configurations

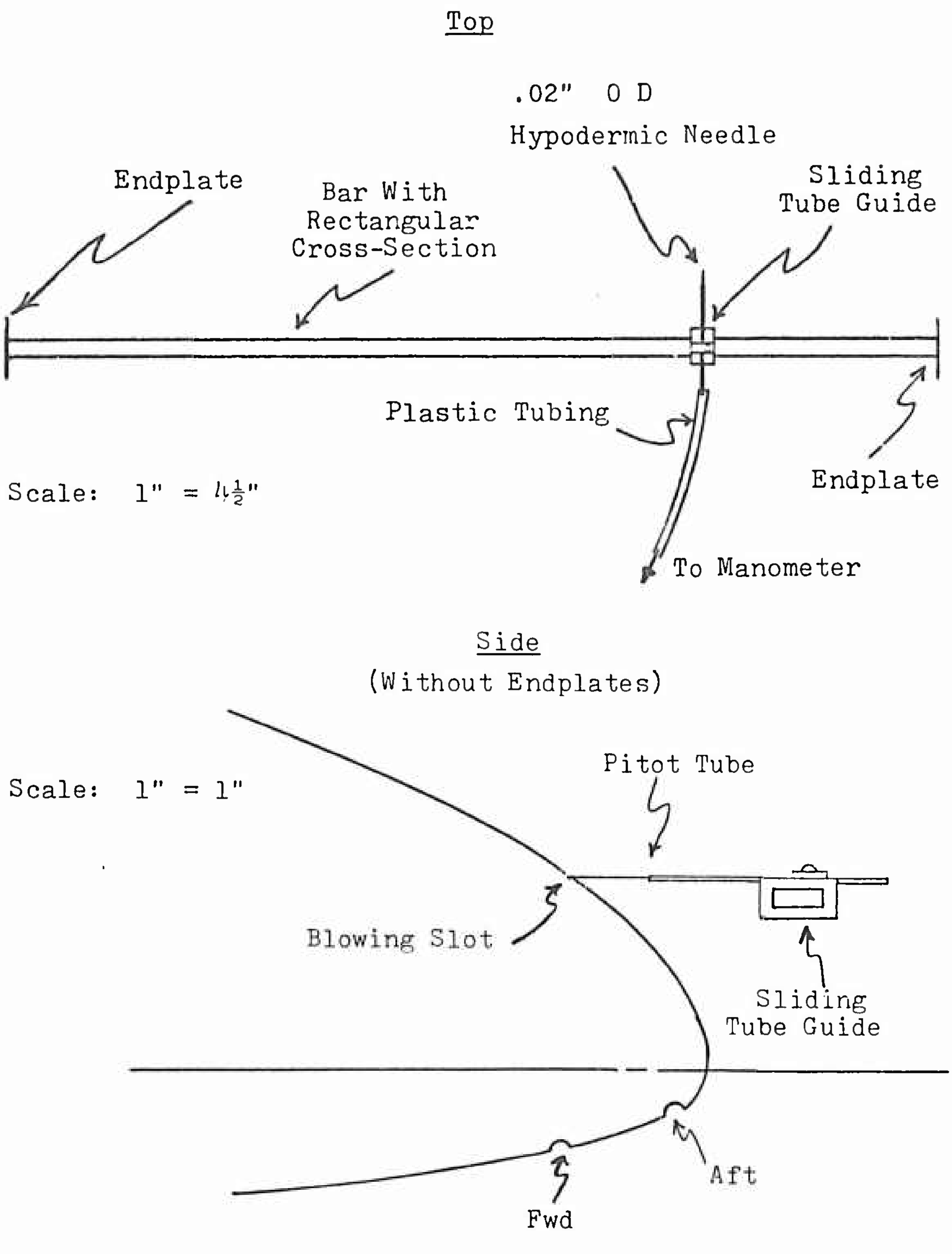

Fig. 5. Pitot Tube Apparatus

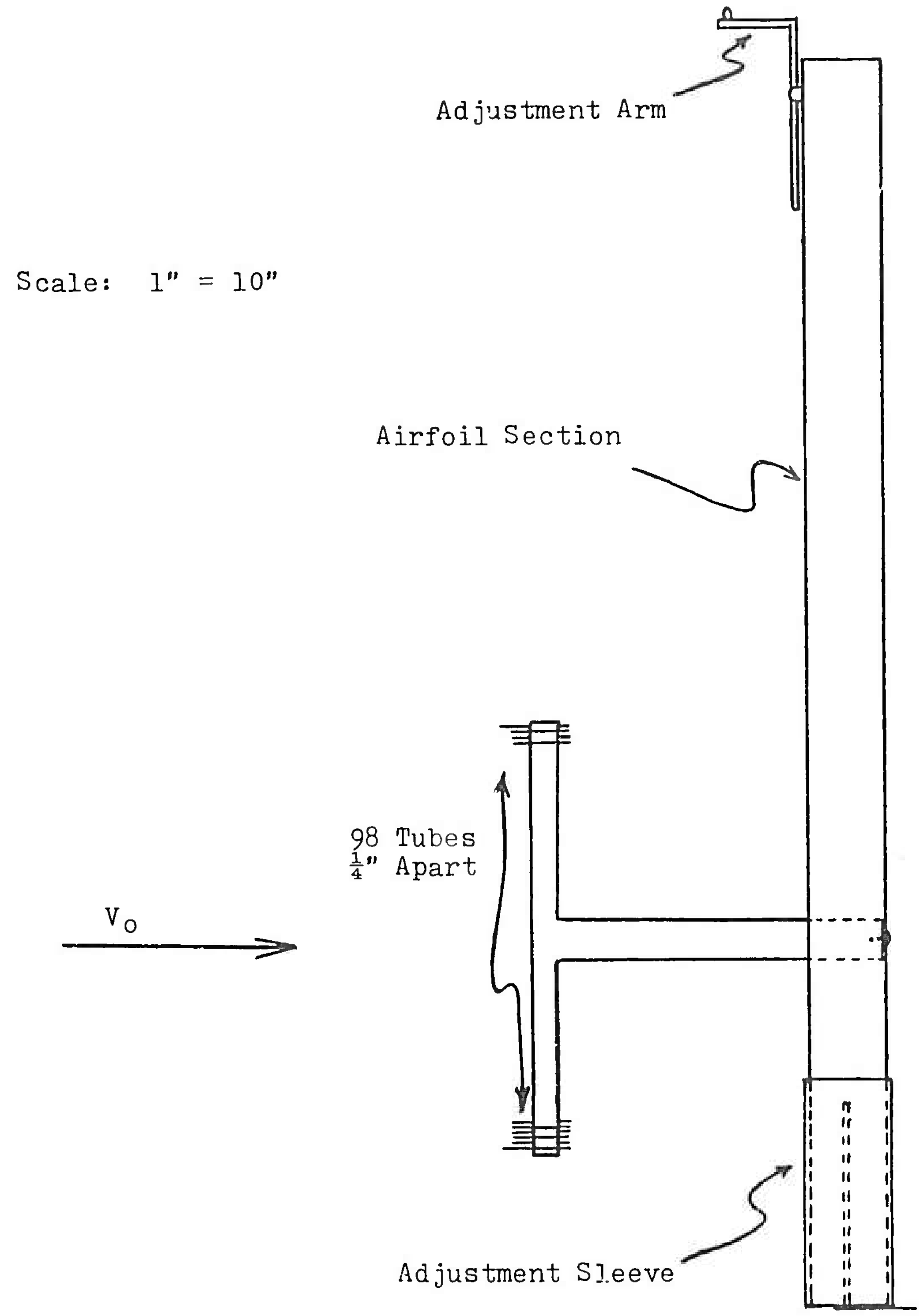

Fig. 6. Wake Survey Rake

Appendix B

Tabulated Data

Table I

Spanwise Total Pressure Distribution at the Blowing Slot

	C_μ = .038	C_μ = .060	C_μ = .090
z in.	P_t in. Hg (guage)	P_t in. Hg (guage)	P_t in. Hg (guage)
1	1.3	1.6	3.2
2	1.3	1.8	3.2
3	1.4	1.8	3.4
4	1.4	2.0	3.5
5	1.4	2.0	3.6
6	1.4	1.9	3.5
7	1.4	2.0	3.6
8	1.3	2.0	3.7
9	1.4	2.0	3.7
10	1.4	2.0	3.7
11	1.4	2.0	3.6
12	1.4	2.0	3.7
13	1.4	2.0	3.7
14	1.4	2.0	3.7
15	1.4	2.0	3.7
16	1.4	2.0	3.7
17	1.4	2.0	3.7
18	1.3	1.8	3.7
19	1.3	1.9	3.7
20	1.3	1.8	3.7
21	1.3	1.8	3.6
22	1.3	1.8	3.6
23	1.3	1.9	3.6
24	1.3	1.9	3.7
25	1.3	1.9	3.7
26	1.3	1.8	3.7

z - Distance from the left endplate measured in inches.

Table II

Airfoil Splitter Plate Configurations in Order of Decreasing C_ℓ Attained at $C_\mu = 0.04$ and $\alpha_g = -2^\circ$

Order	Configuration β	Configuration Position	C_ℓ	% Improvement Over Clean Configuration
1	60°	aft	2.60	99%
2	45°	aft	2.37	81%
3	60°	forward	2.36	80%
4	45°	forward	2.21	69%
5	30°	aft	1.83	40%
6	none	none	1.31	0%

Table III

Airfoil Splitter Plate Configurations in Order of Increasing C_{d_t} Attained at $C_\mu = 0.04$ and $\alpha_g = -2^\circ$

Order	Configuration β	Configuration Position	C_{d_t}	% Change From Clean Configuration
1	45°	aft	.049	- 9%
2	30°	aft	.051	- 6%
3	none	none	.054	0%
4	60°	forward	.057	+ 6%
5	45°	forward	.062	+15%
6	60°	aft	.063	+17%

Table IV

Airfoil Splitter Plate Configurations in Order of Decreasing ℓ/d Attained at $C_\mu = 0.04$ and $\alpha_g = -2^\circ$

Order	Configuration β	Configuration Position	ℓ/d	% Improvement Over Clean Configuration
1	45°	aft	48	92%
2	60°	aft	42	68%
3	60°	forward	42	68%
4	45°	forward	40	60%
5	30°	aft	36	44%
6	none	none	25	0%

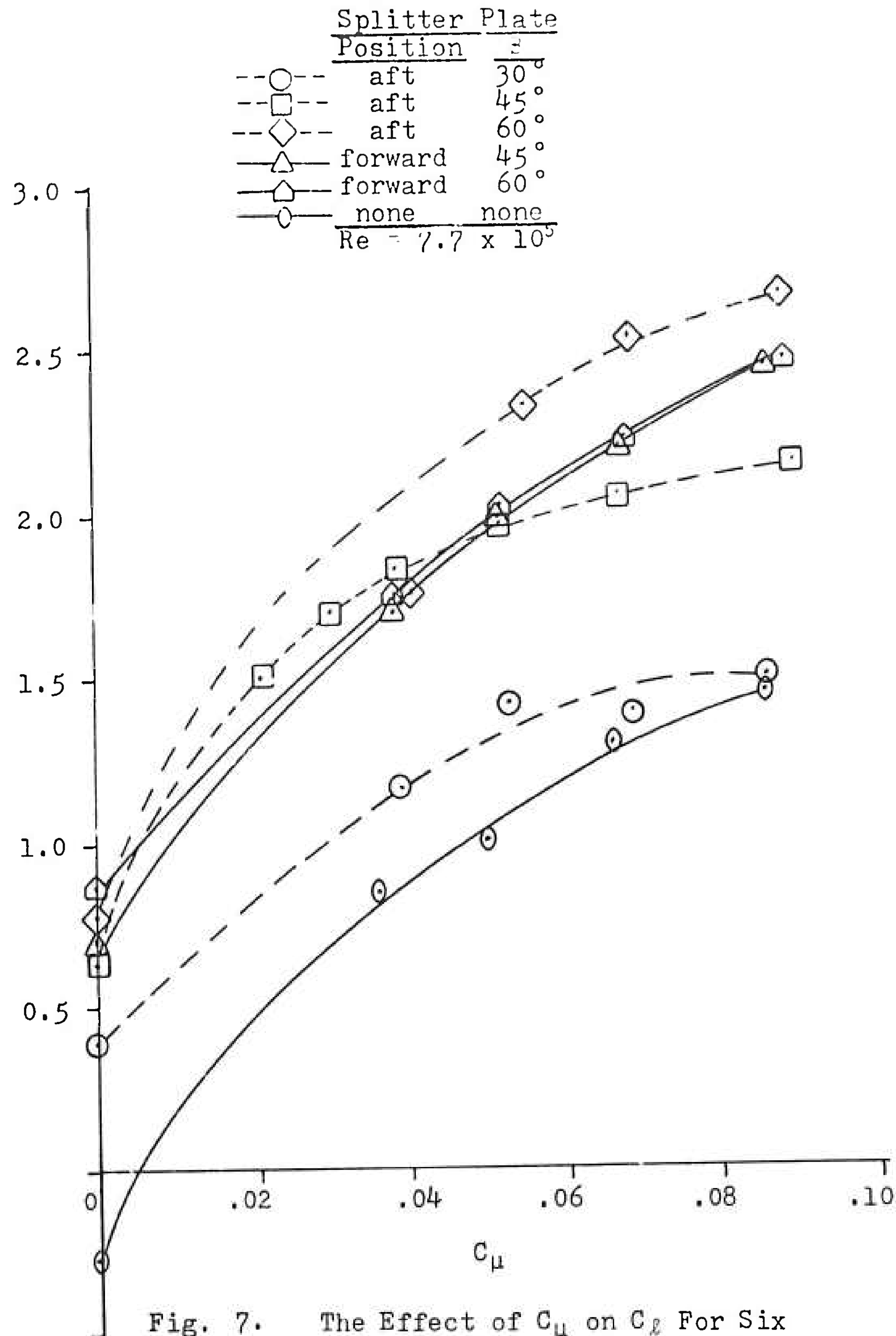

Fig. 7. The Effect of C_μ on C_ℓ For Six Airfoil Splitter Plate Configurations at an α_g of -6 Degrees

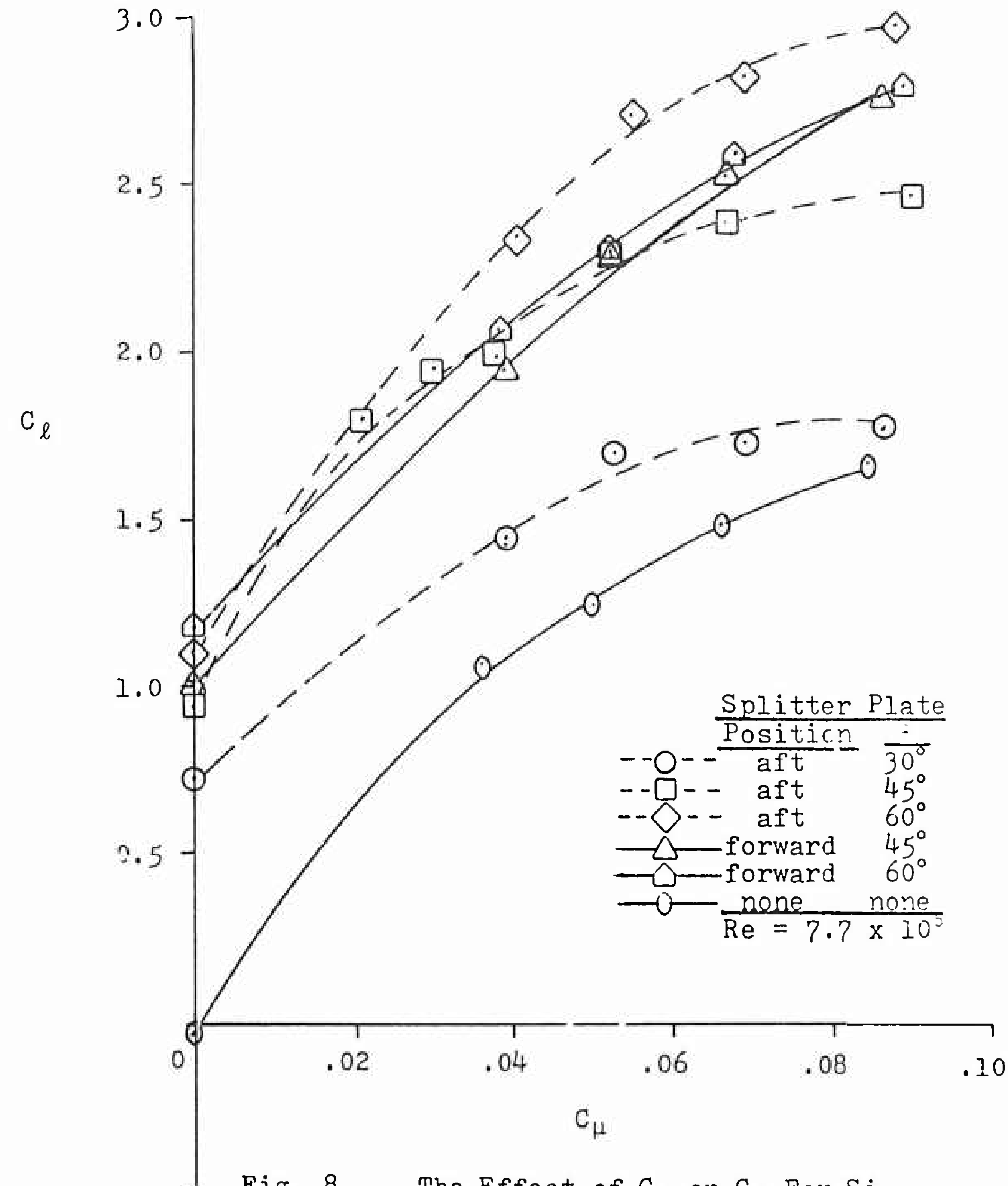

Fig. 8. The Effect of C_μ on C_ℓ For Six Airfoil Splitter Plate Configurations at an α_g of -4 Degrees

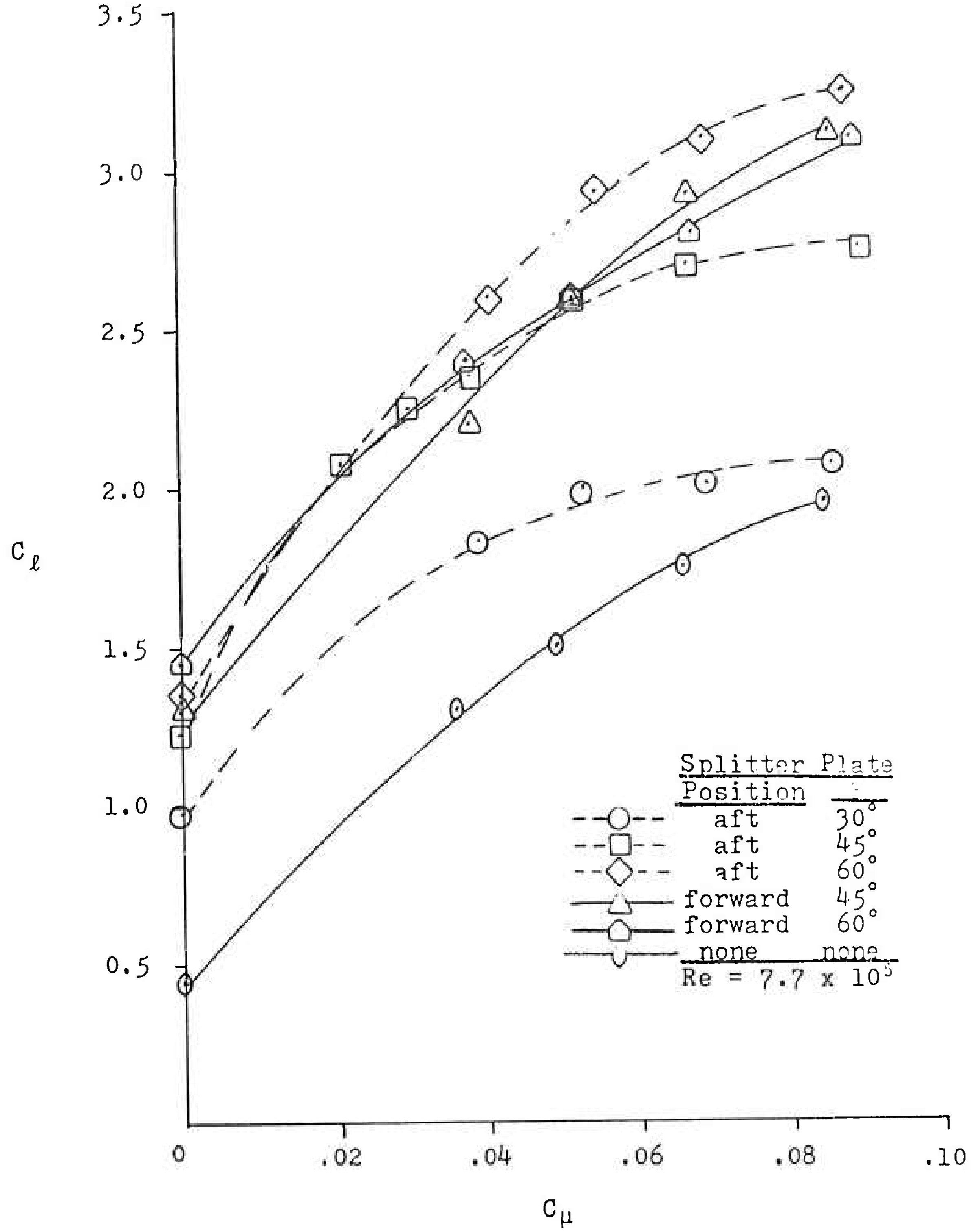

Fig. 9. The Effect of C_μ on C_ℓ For Six Airfoil Splitter Plate Configurations at an α_g of -2 Degrees

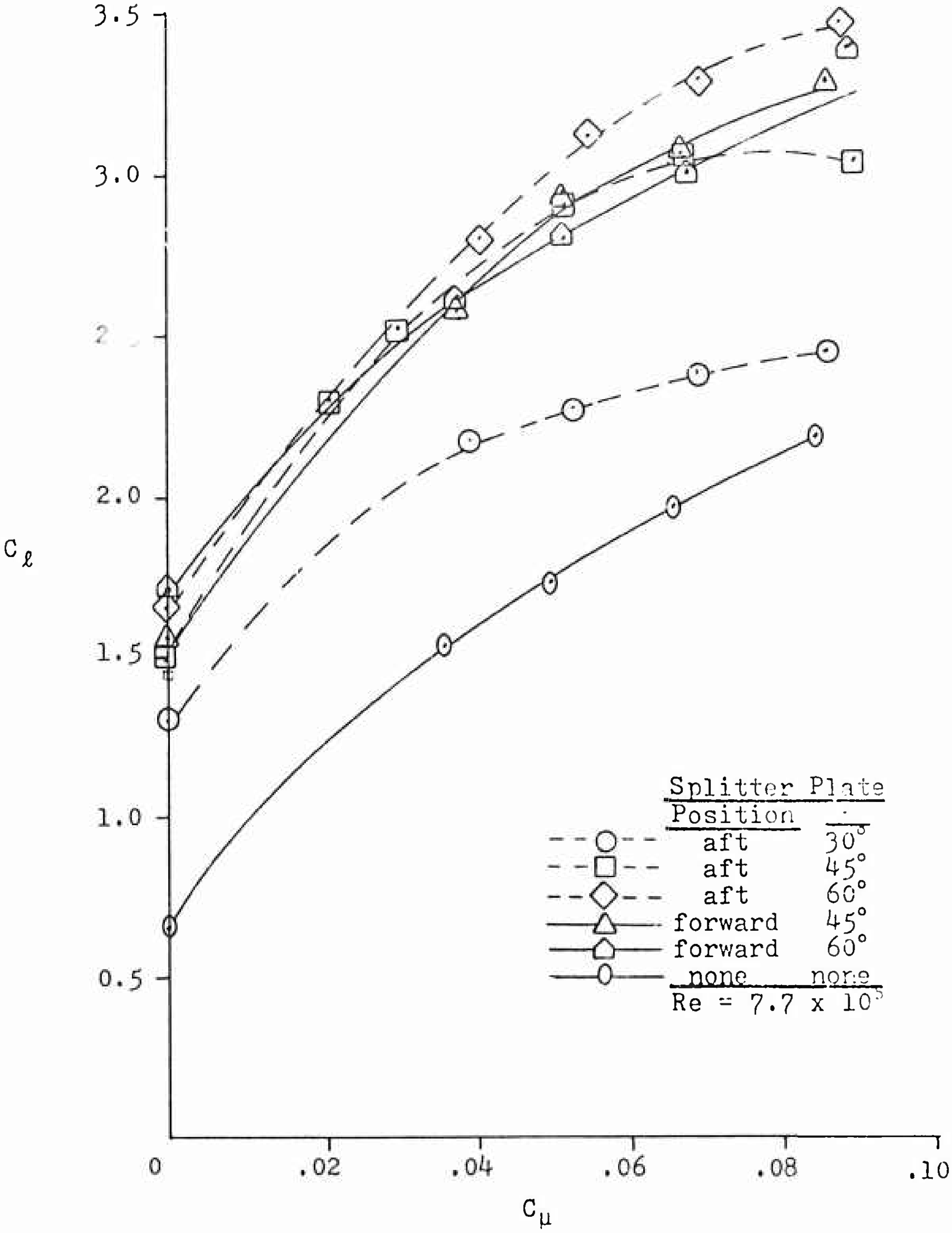

Fig. 10. The Effect of C_μ on C_ℓ For Six Airfoil Splitter Plate Configurations at an α_g of 0 Degrees

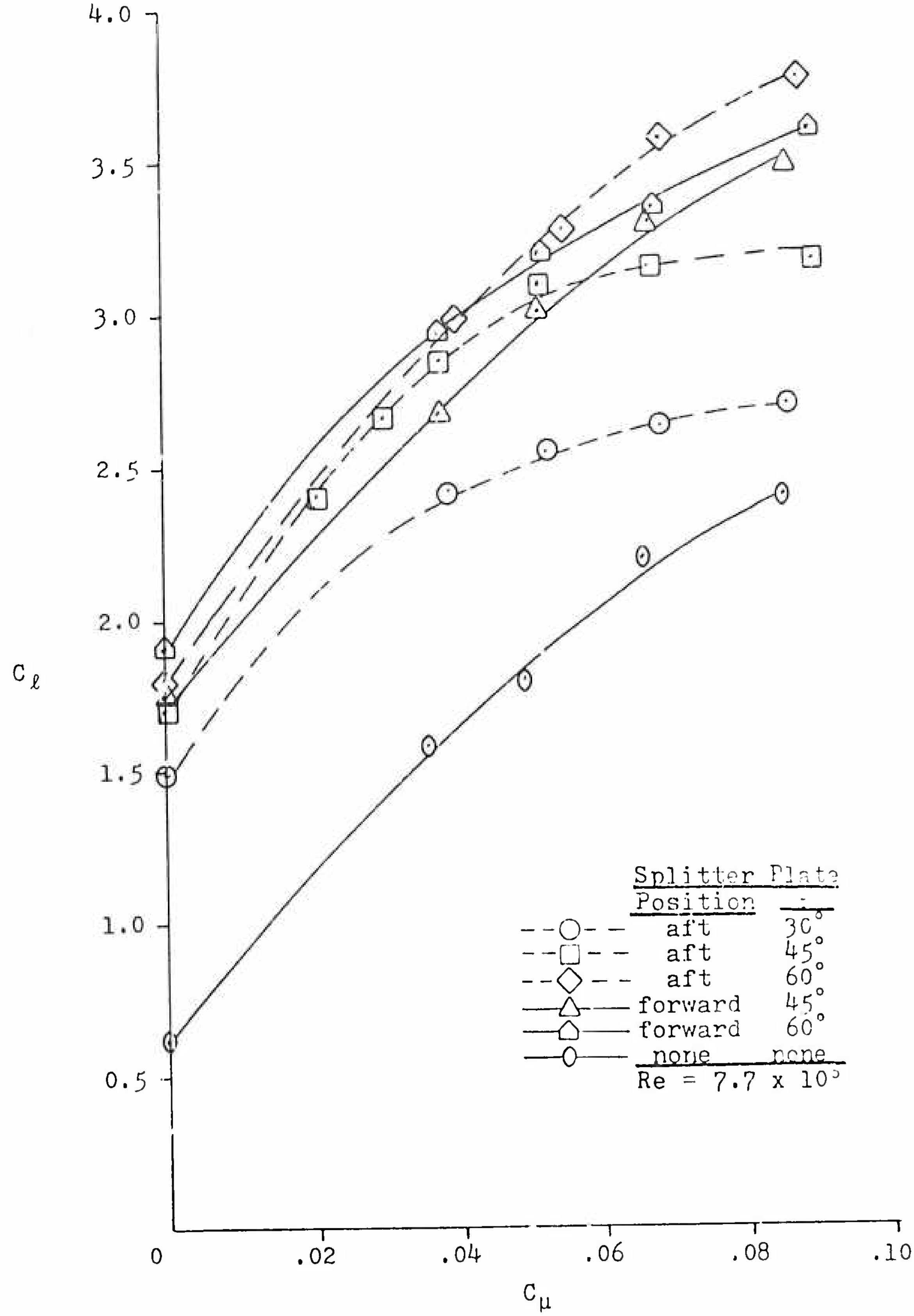

Fig. 11. The Effect of C_μ on C_ℓ For Six Airfoil Splitter Plate Configurations at an α_g of +2 Degrees

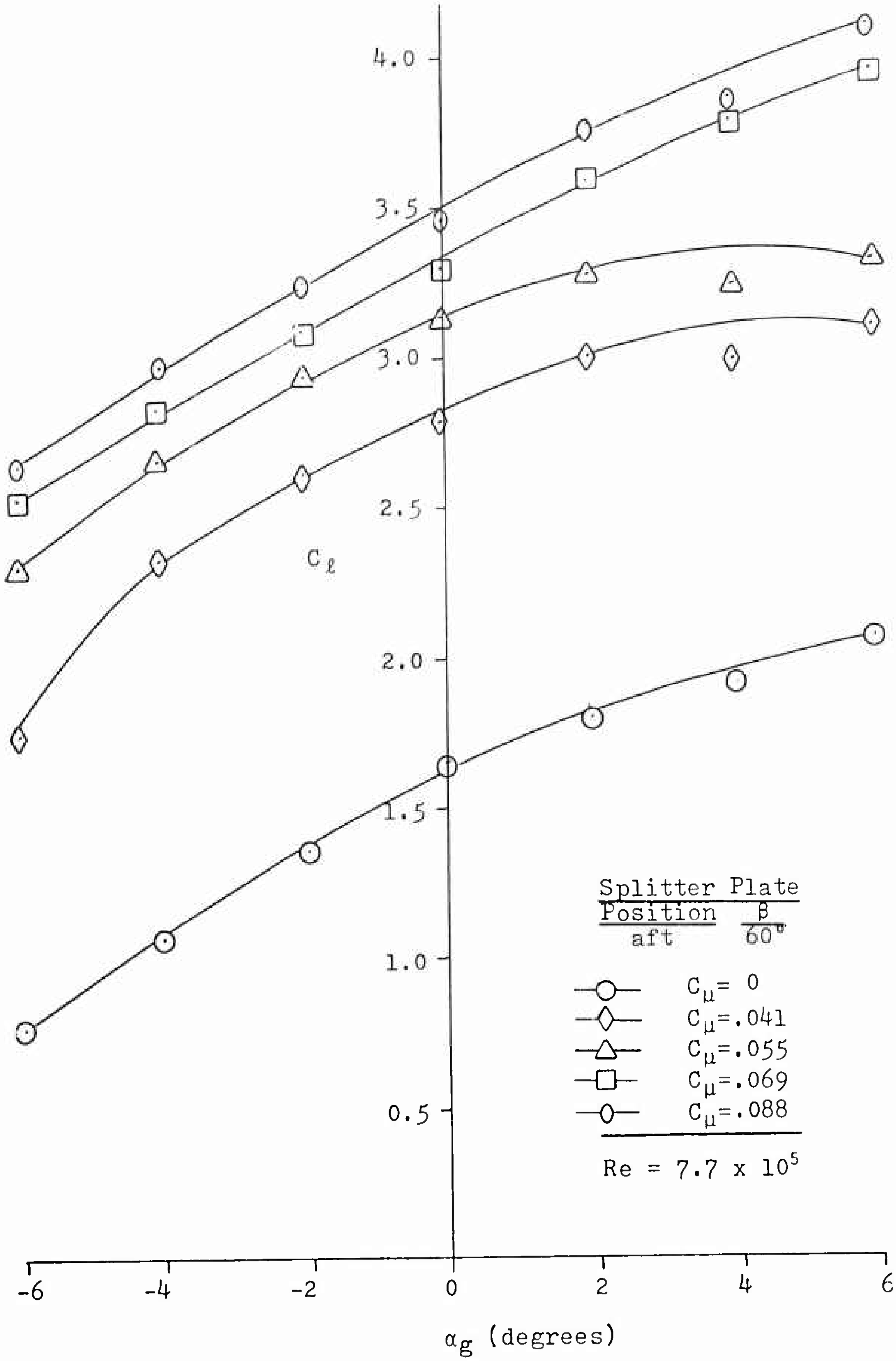

Fig. 12. The Effect of α_g on C_ℓ For Five C_μ's

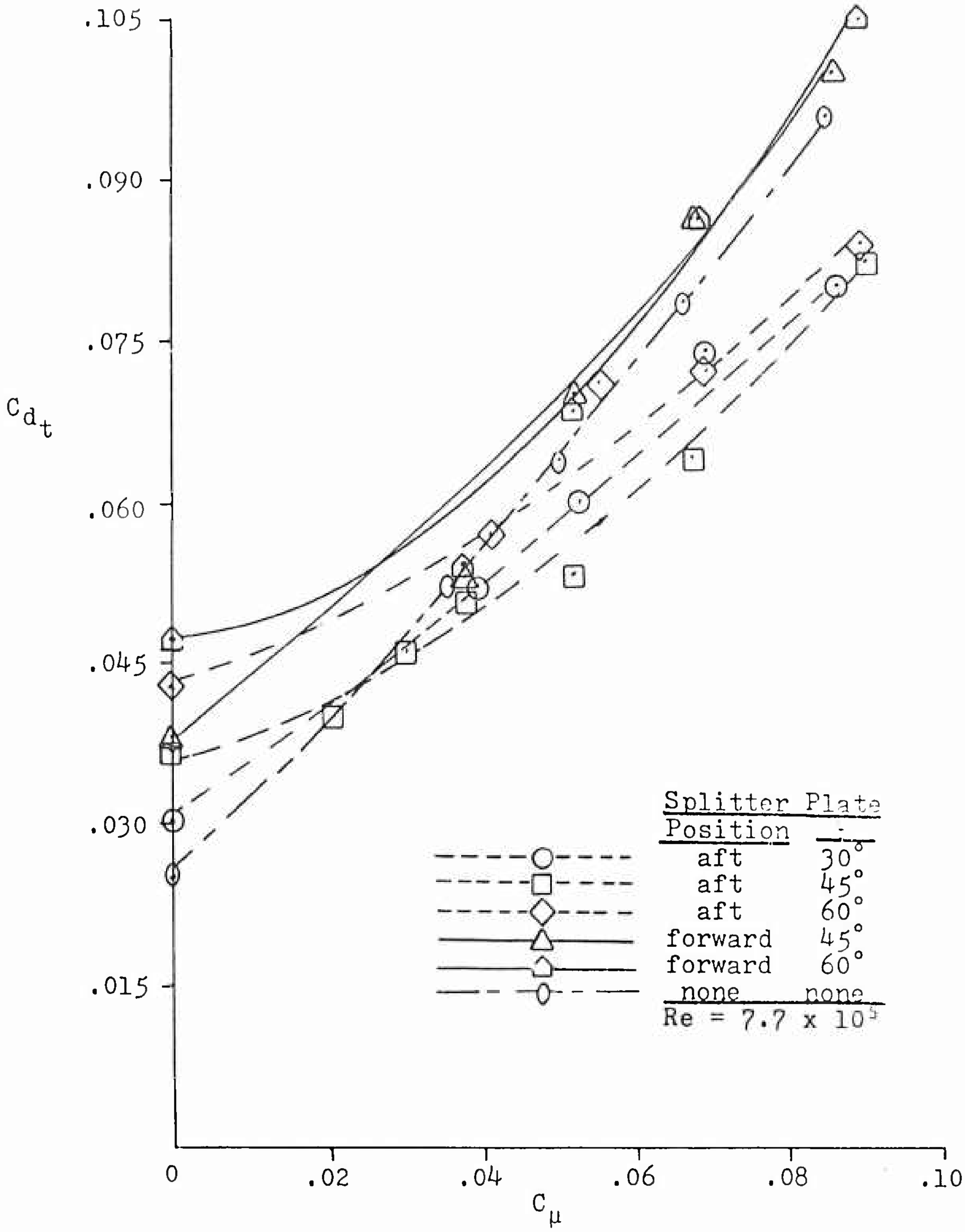

Fig. 13. The Effect of C_μ on C_{d_t} For Six Airfoil Splitter Plate Configurations at an α_g of -6 Degrees

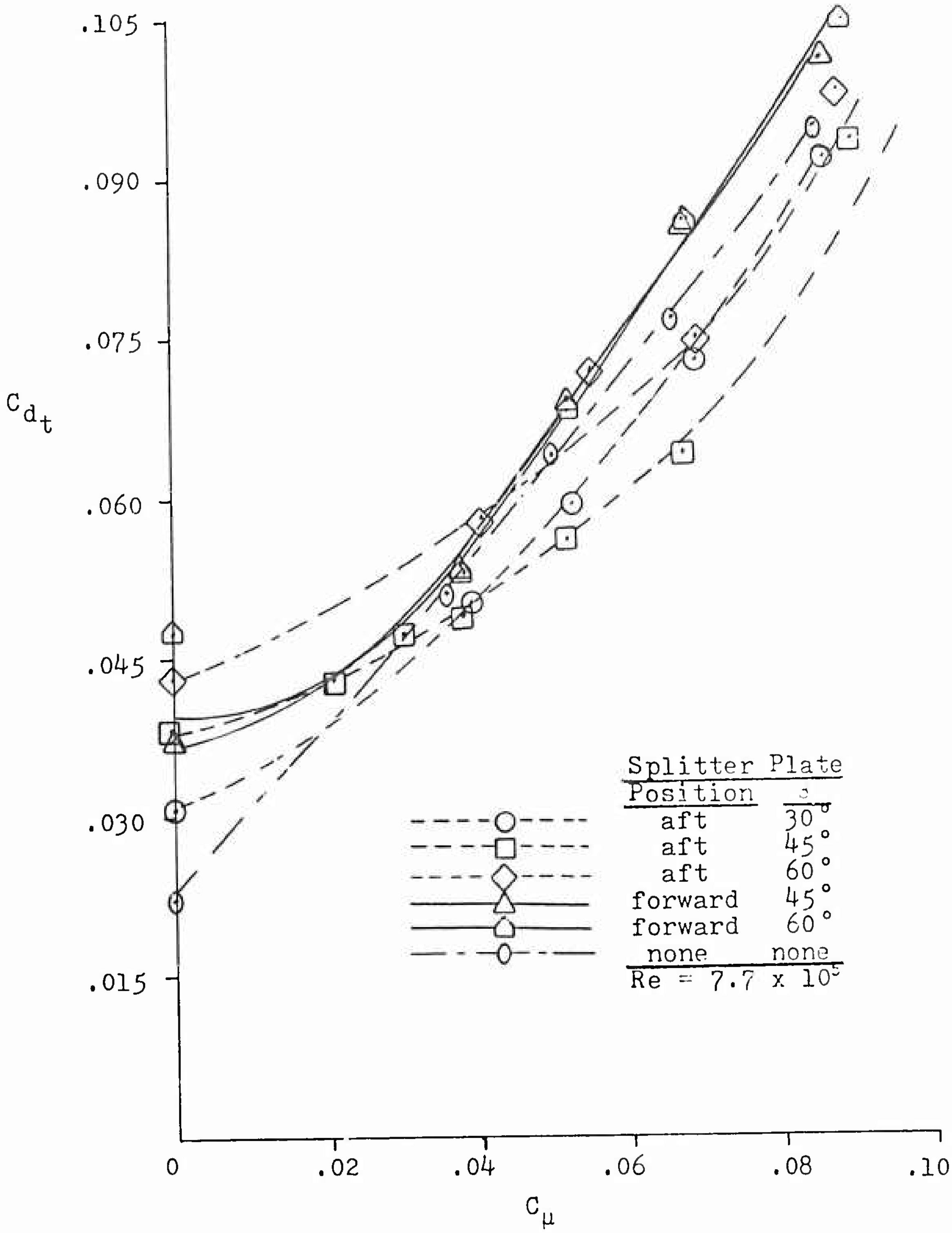

Fig. 14. The Effect of C_μ on C_{d_t} For Six Airfoil Splitter Plate Configurations at an α_g of -4 Degrees

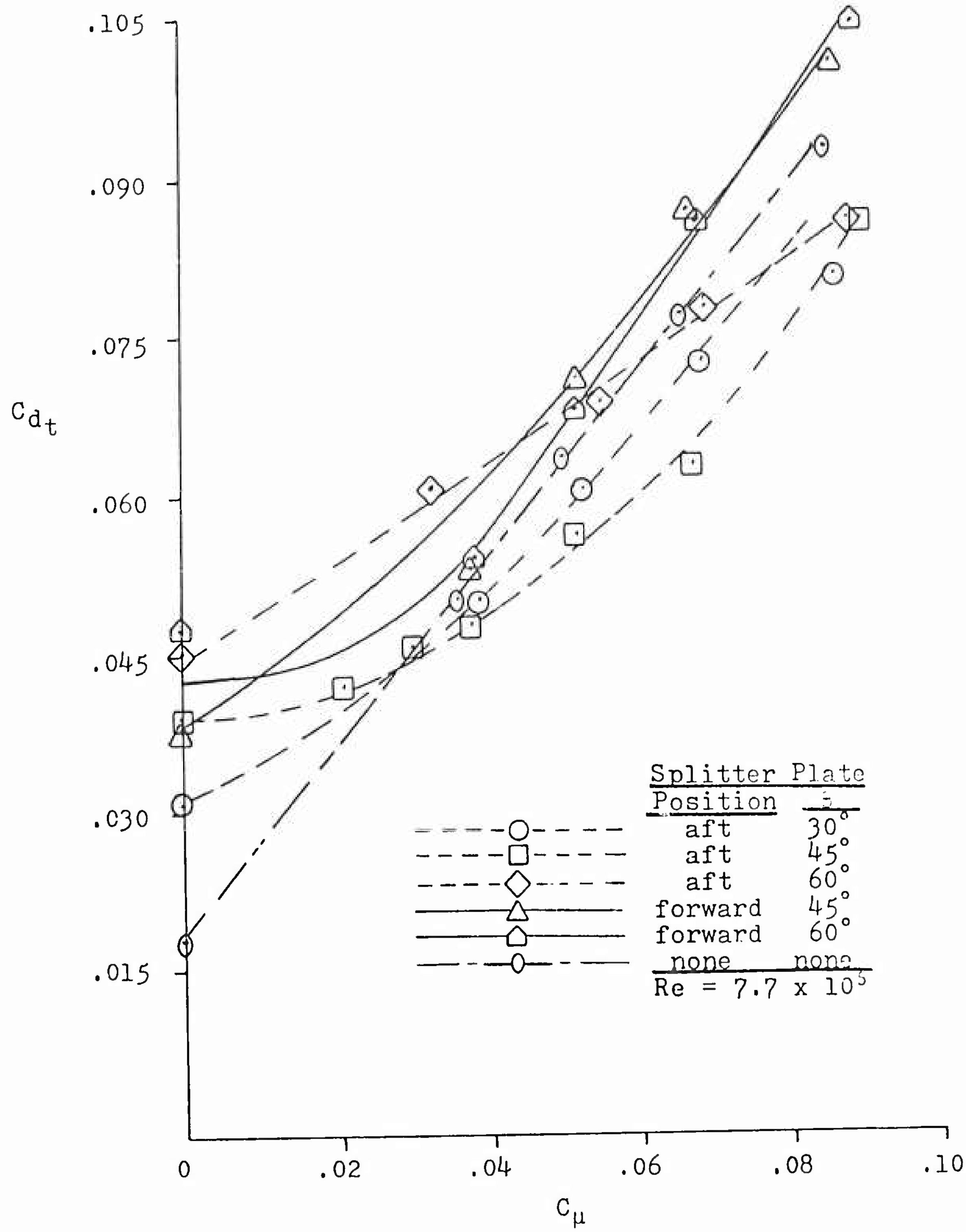

Fig. 15. The Effect of C_μ on C_{d_t} For Six Airfoil Splitter Plate Configurations at an α_g of -2 Degrees

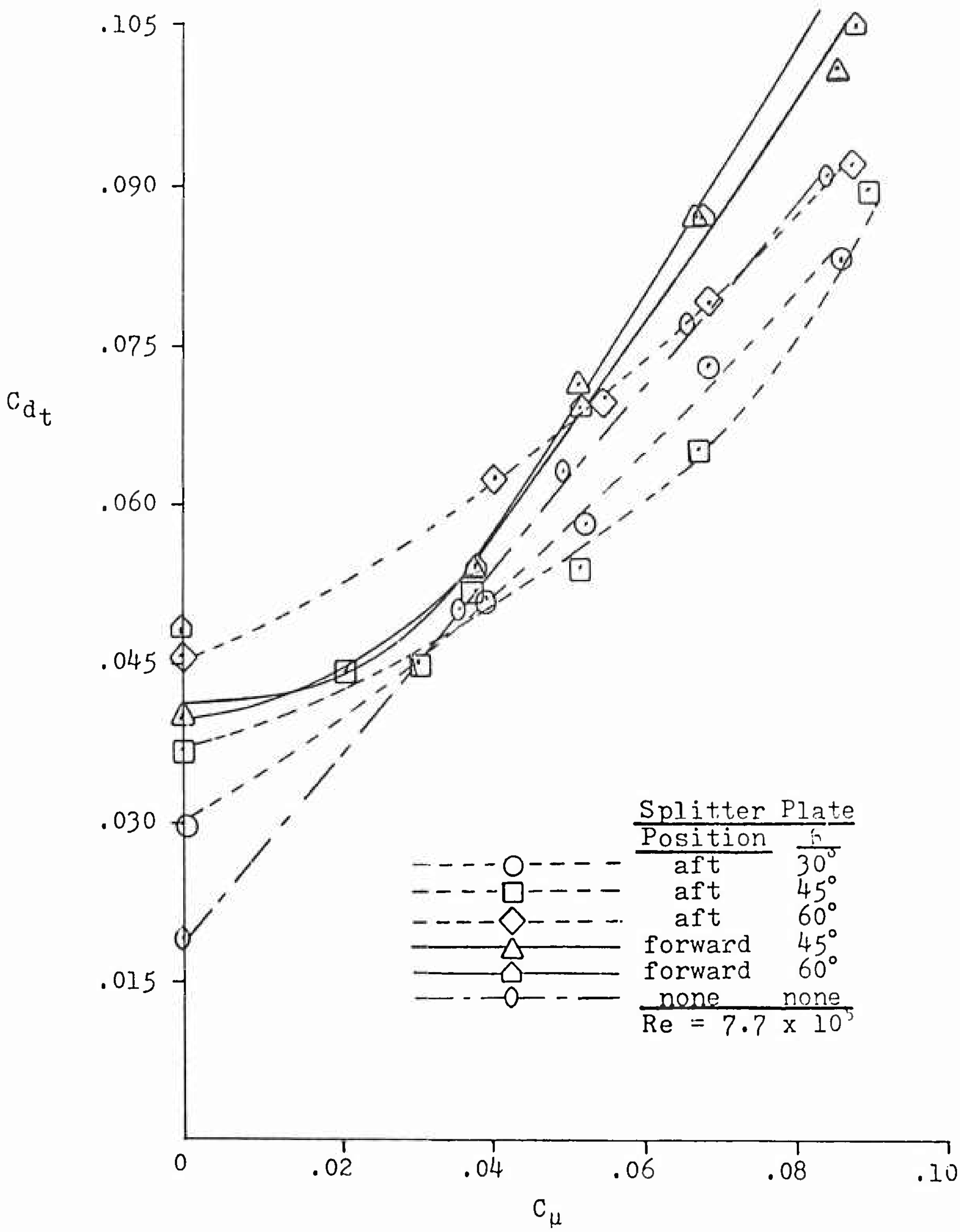

Fig. 16. The Effect of C_μ on C_{d_t} For Six Airfoil Splitter Plate Configurations at an α_g of 0 Degrees

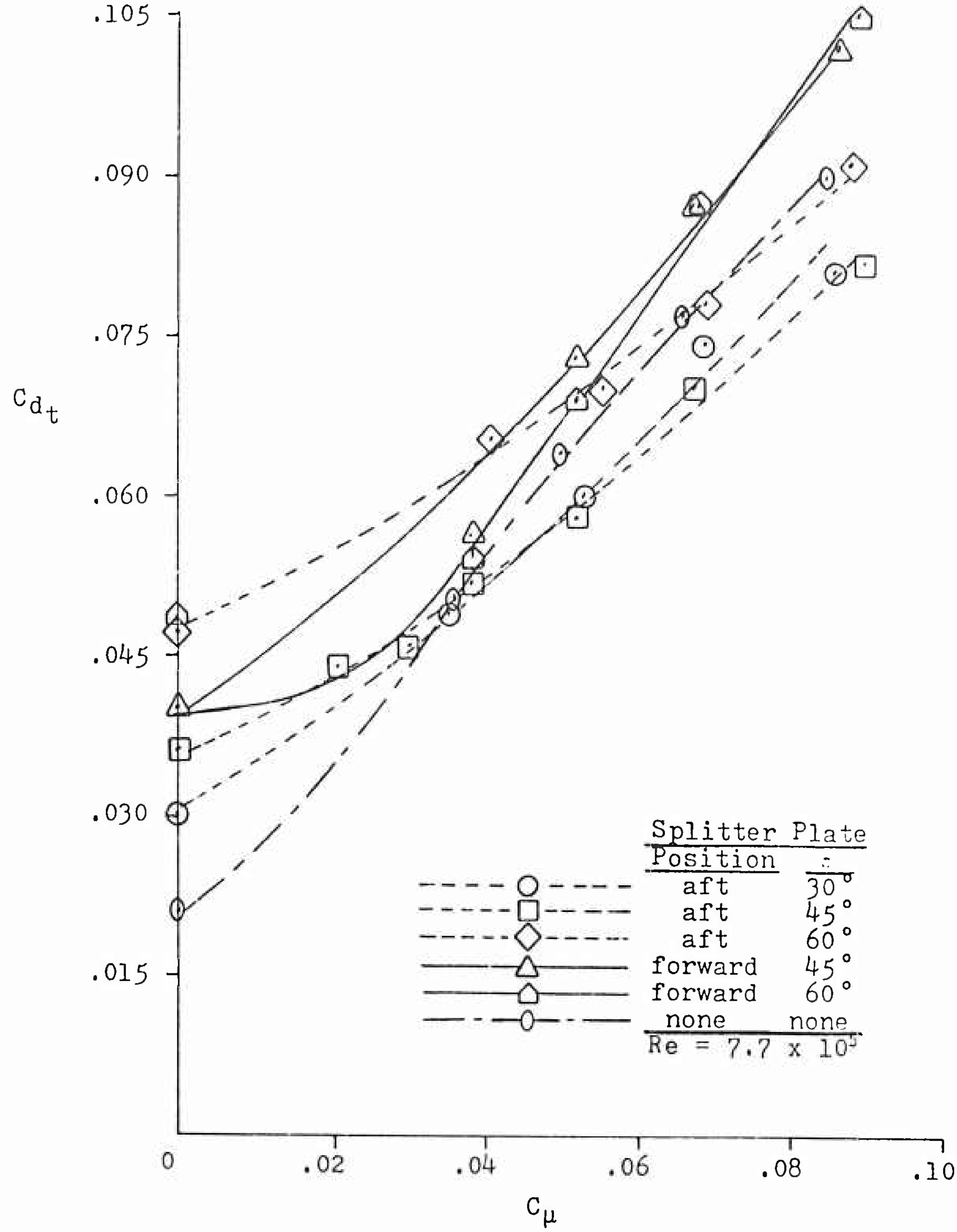

Fig. 17. The Effect of C_μ on C_{d_t} For Six Airfoil Splitter Plate Configurations at an α_g of +2 Degrees

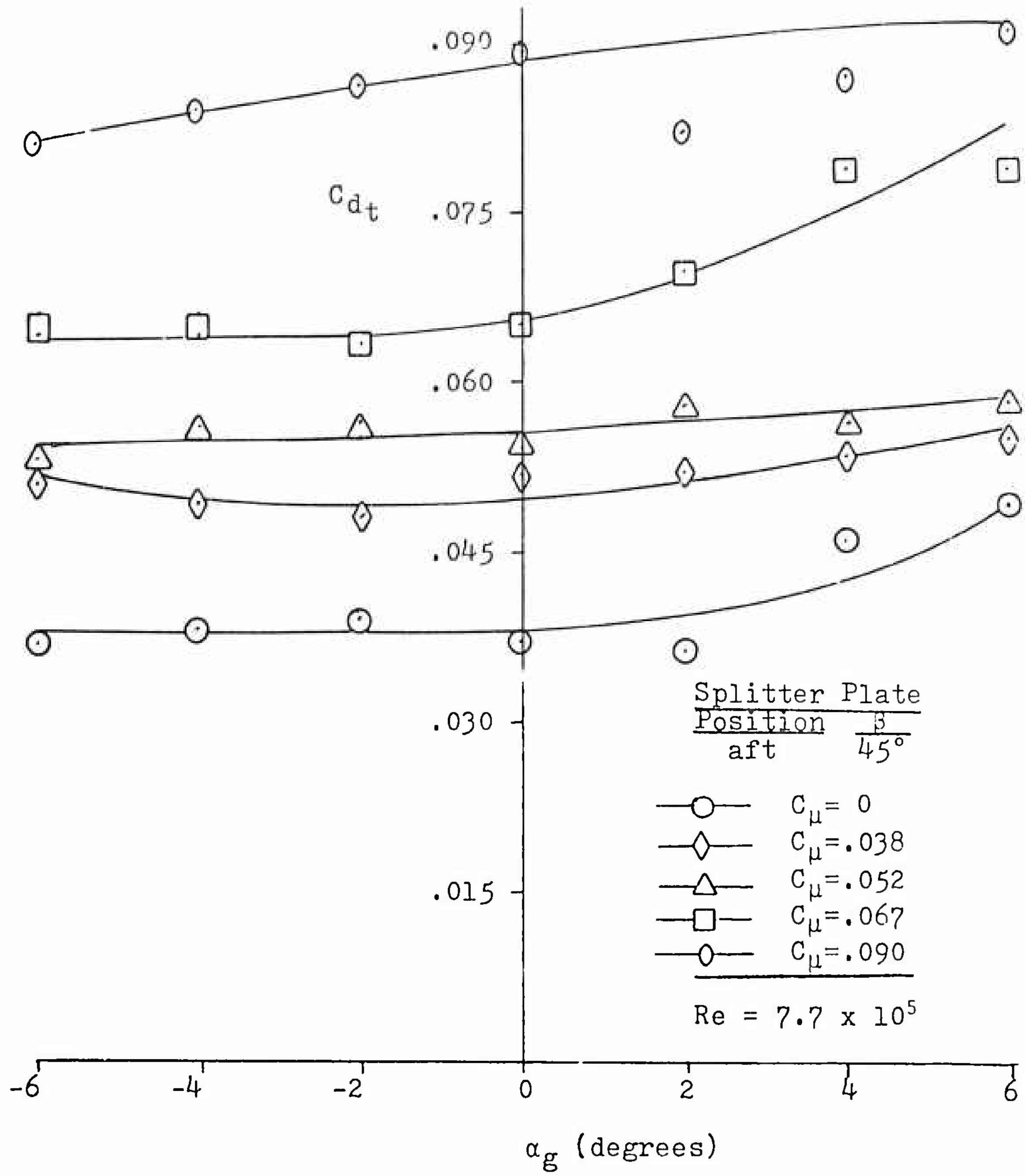

Fig. 18. The Effect of α_g on C_{d_t} For Five C_μ's

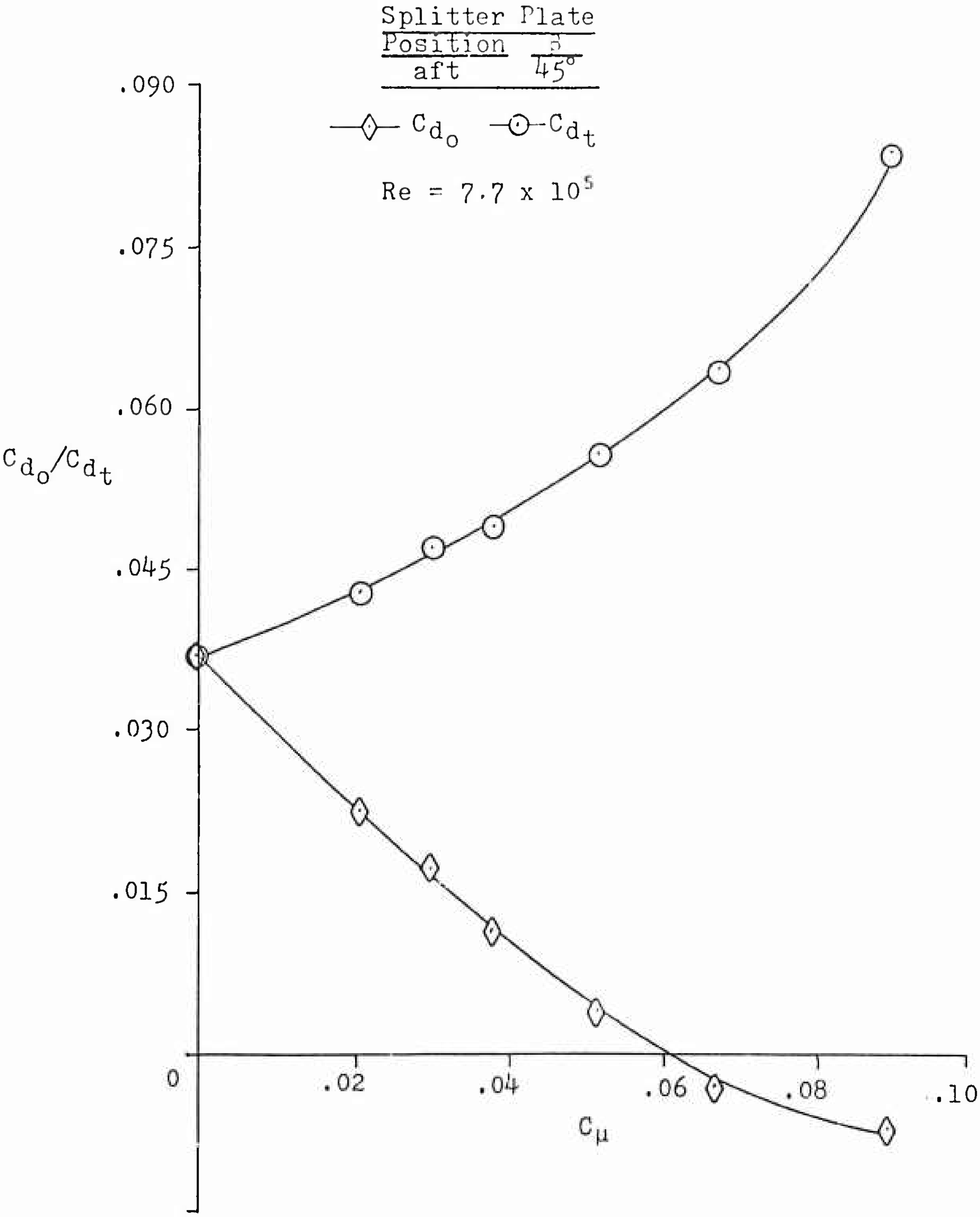

Fig. 19. The Effect of C_μ on C_{d_o} and C_{d_t} at an α_g of -4 Degrees

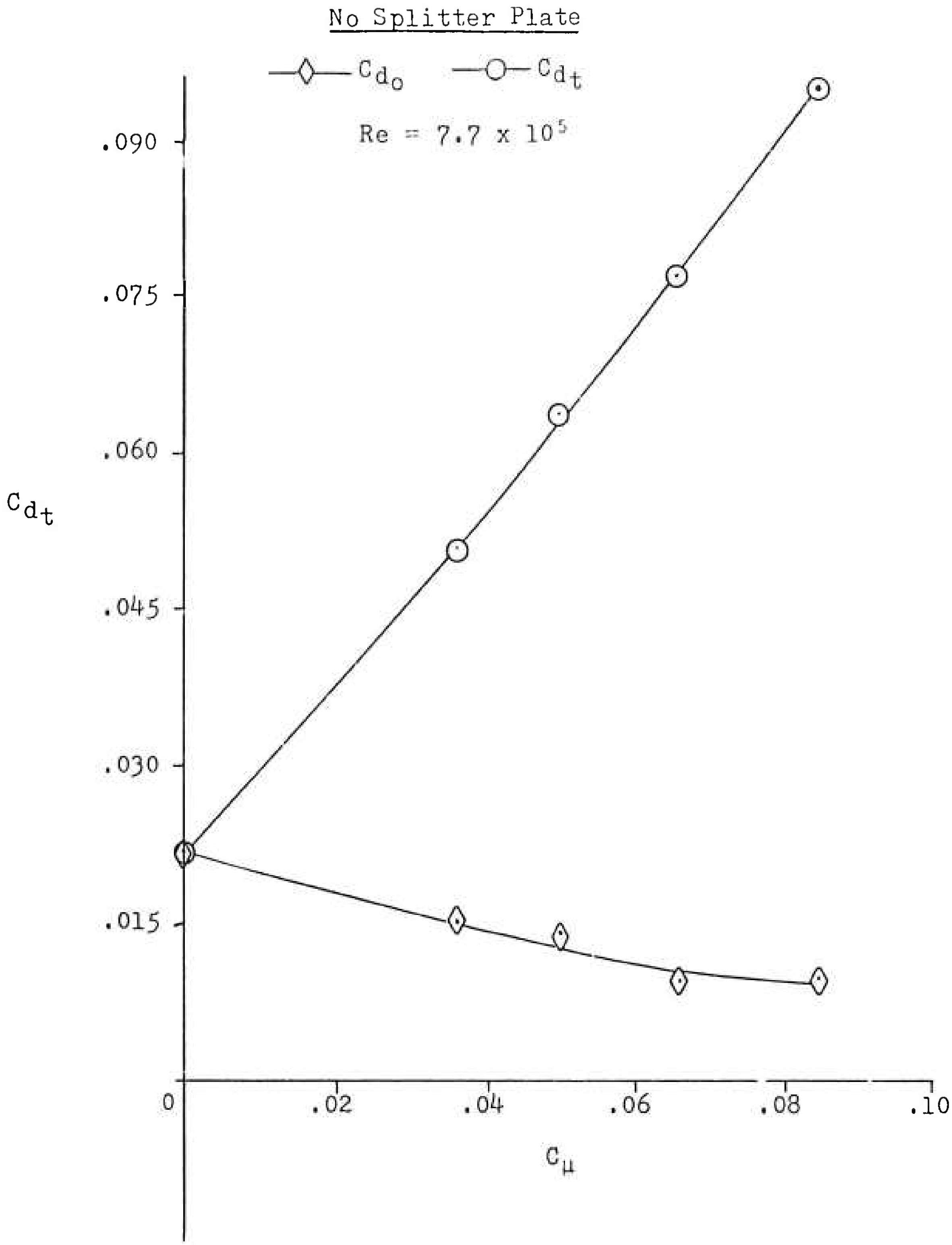

Fig. 20. The Effect of C_μ on C_{d_o} and C_{d_t} at an α_g of -4 Degrees

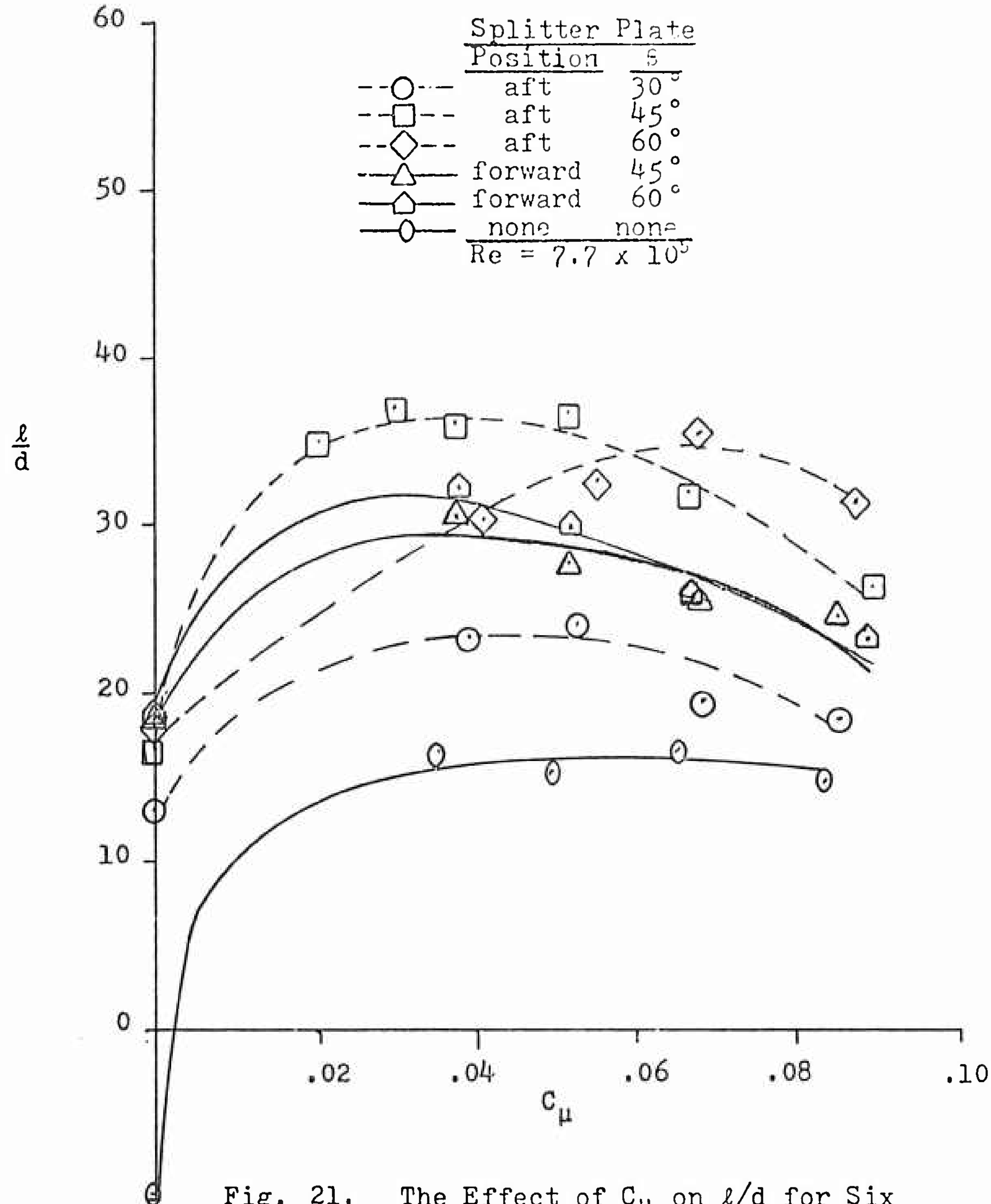

Fig. 21. The Effect of C_μ on ℓ/d for Six Airfoil Splitter Plate Configurations at an α_g of -6 Degrees

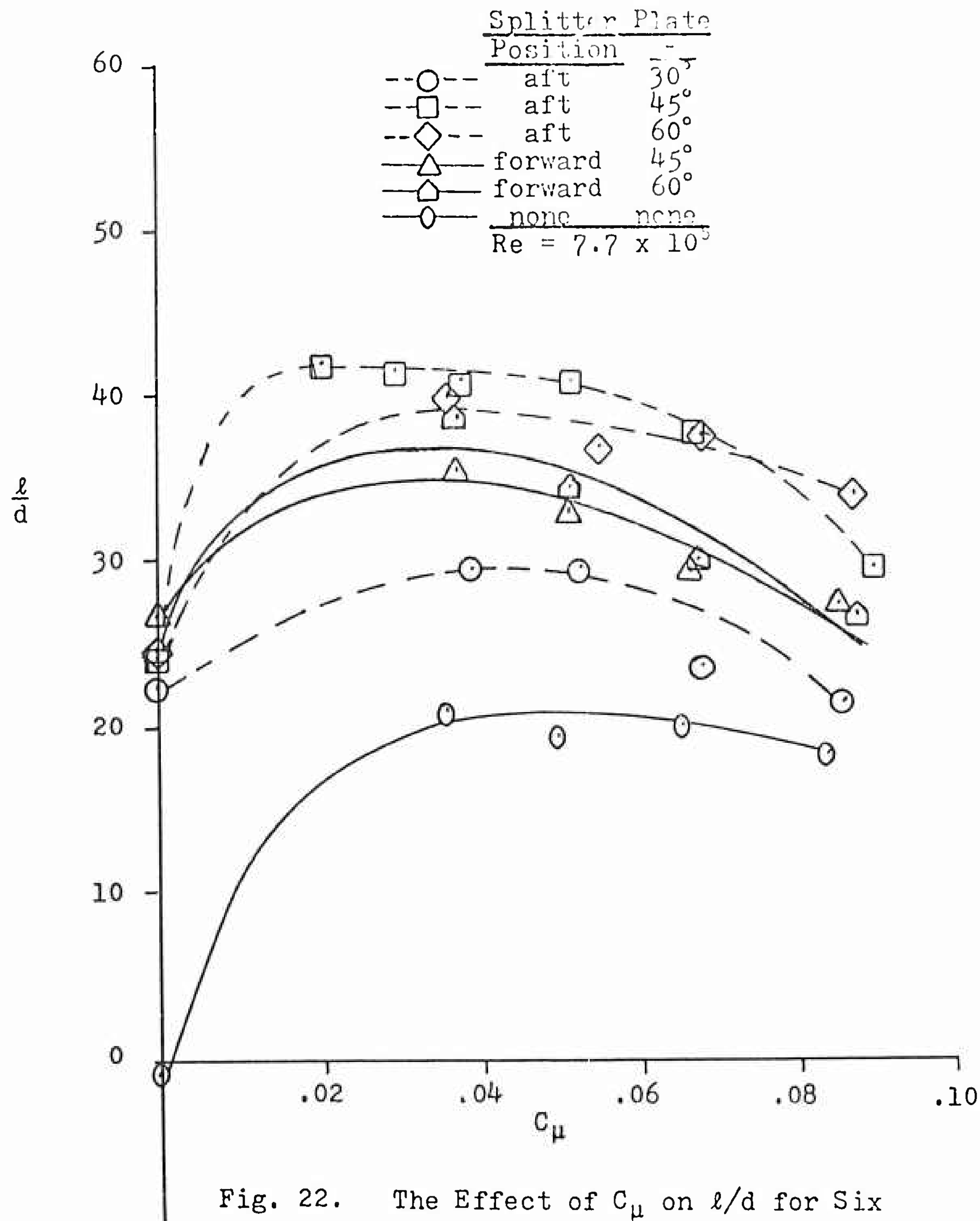

Fig. 22. The Effect of C_μ on ℓ/d for Six Airfoil Splitter Plate Configurations at an α_g of -4 Degrees

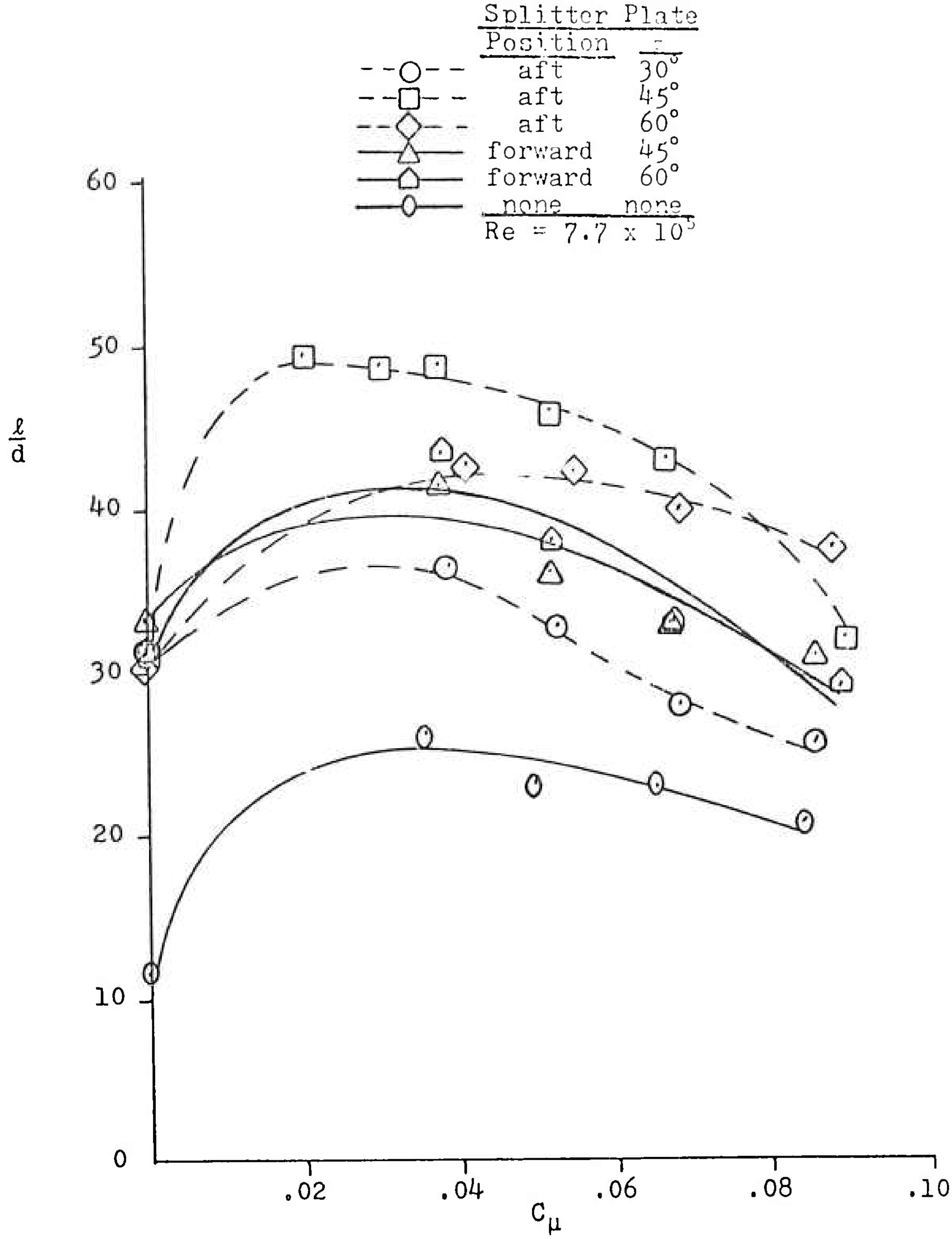

Fig. 23. The Effect of C_μ on ℓ/d for Six Airfoil Splitter Plate Configurations at an α_g of -2 Degrees

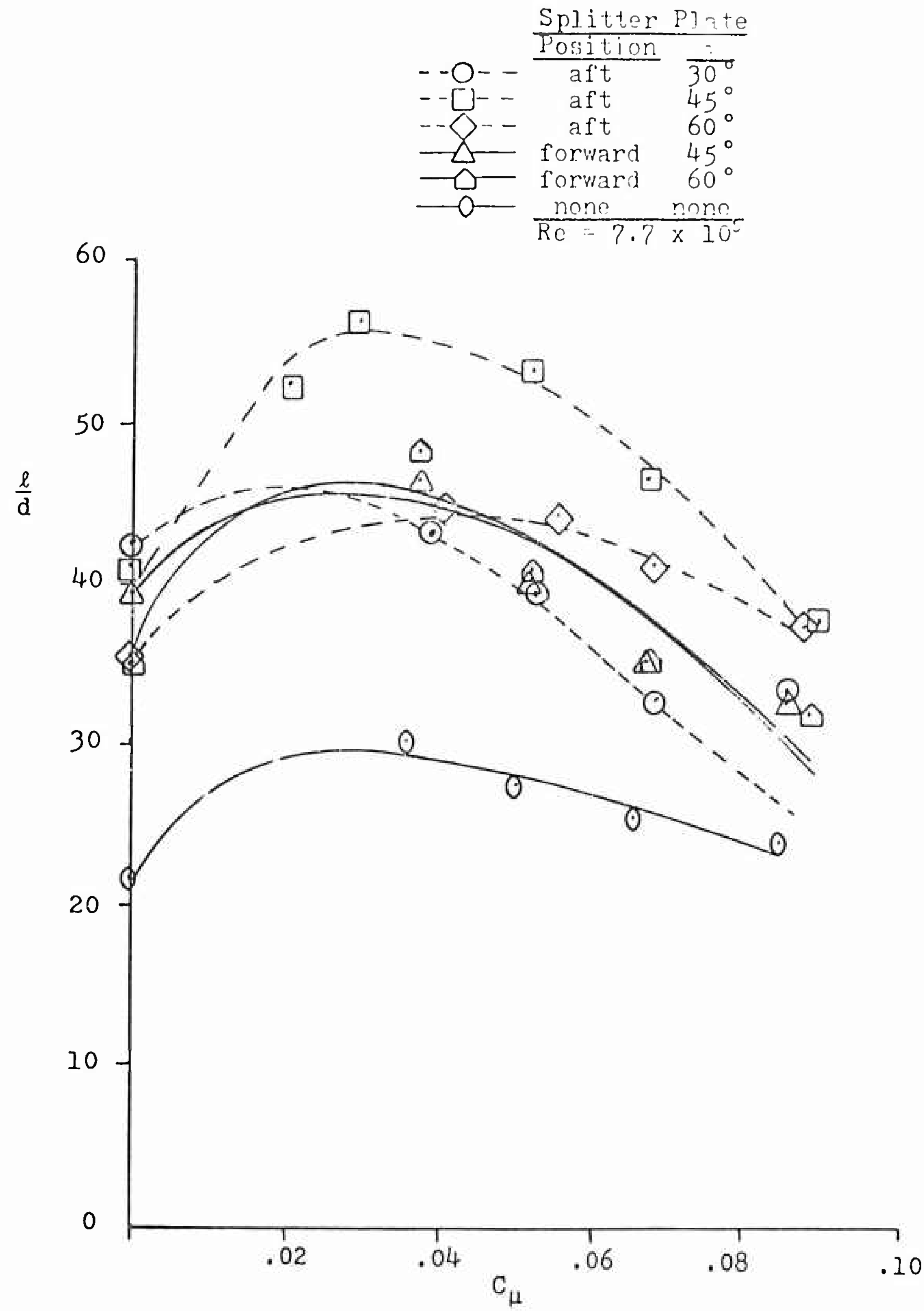

Fig. 24. The Effect of C_μ on ℓ/d for Six Airfoil Splitter Plate Configurations at an α_g of 0 Degrees

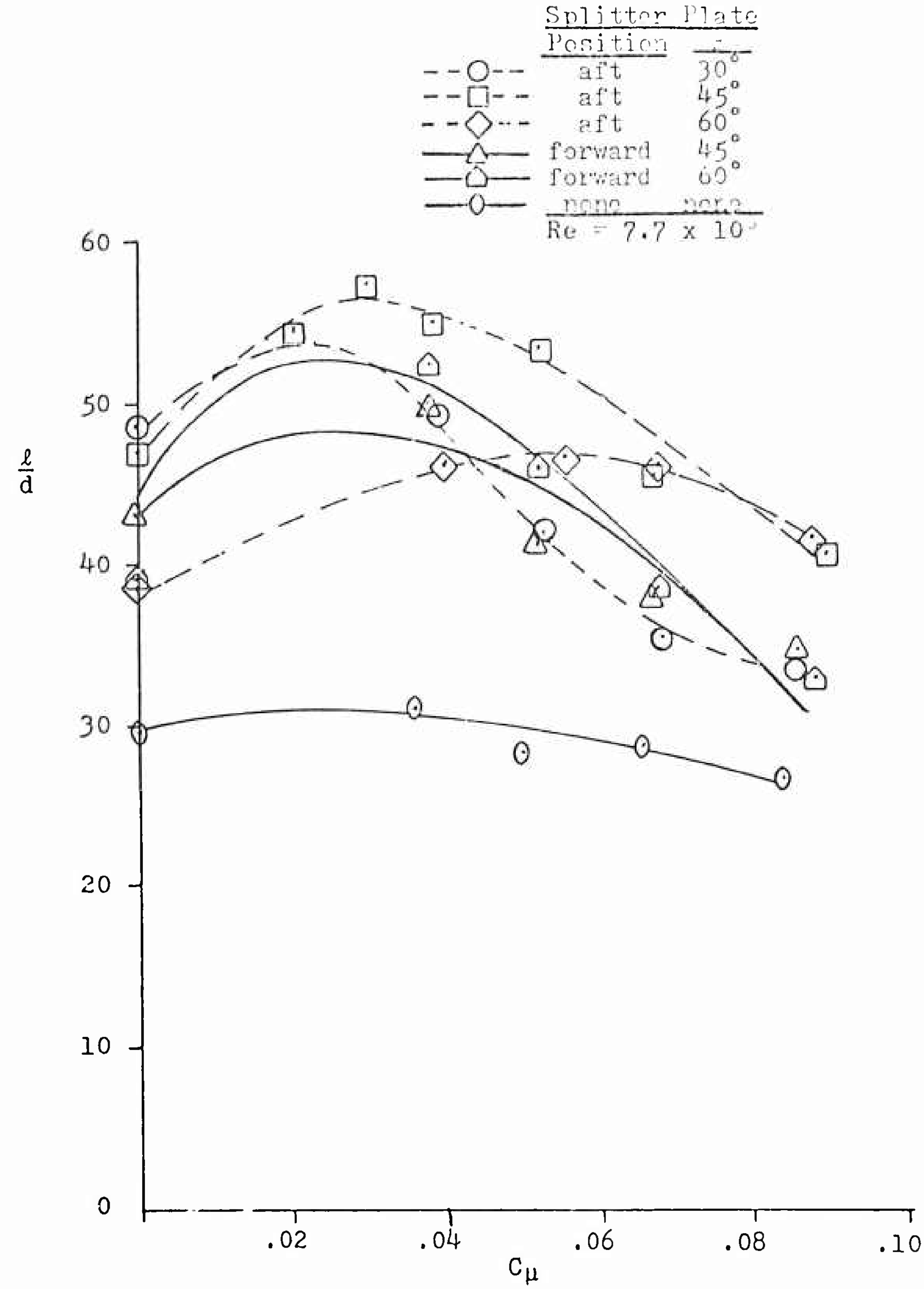

Fig. 25. The Effect of C_μ on ℓ/d for Six Airfoil Splitter Plate Configurations at an α_g of +2 Degrees

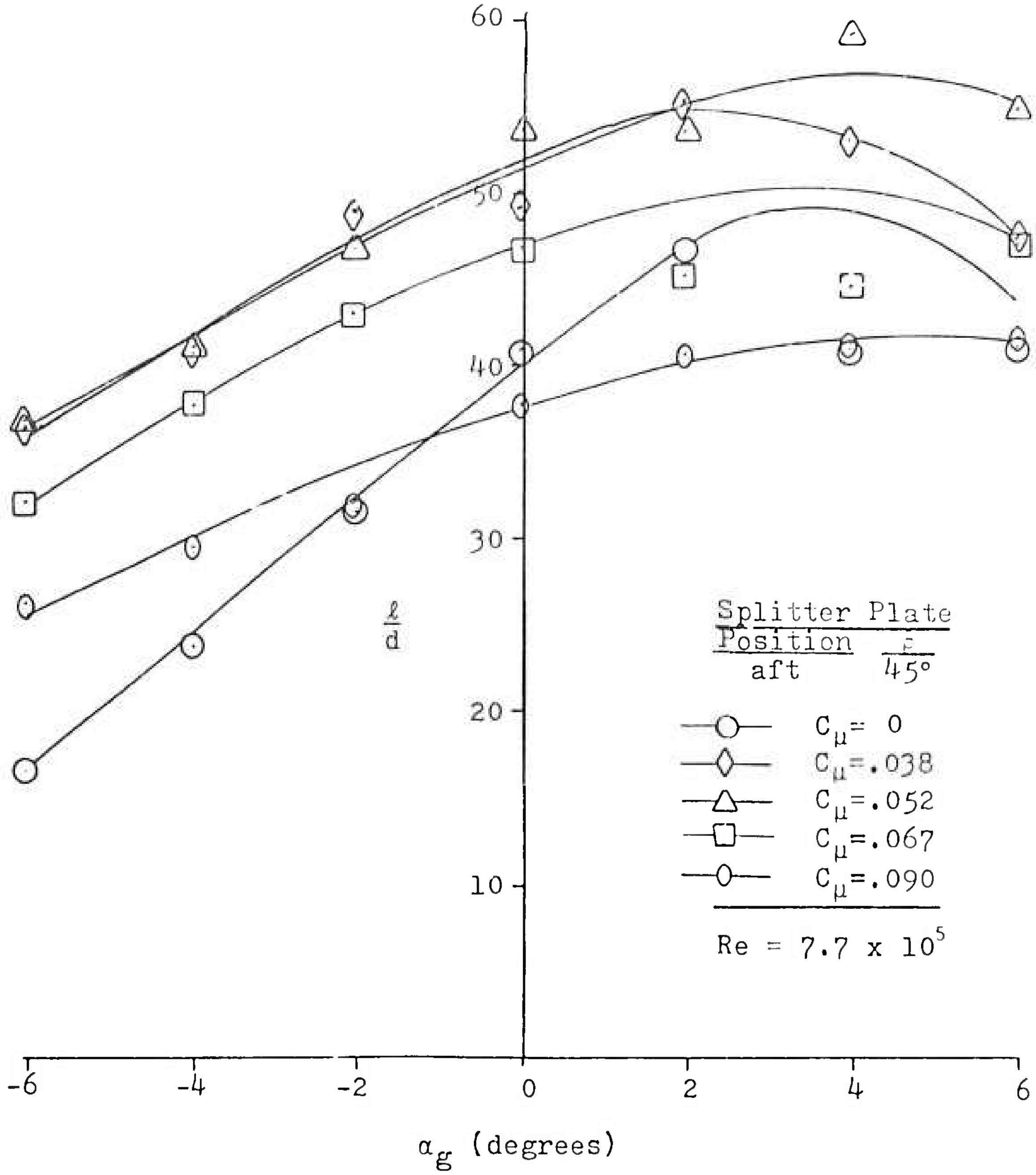

Fig. 26. The Effect of α_g on ℓ/d For Five C_μ's

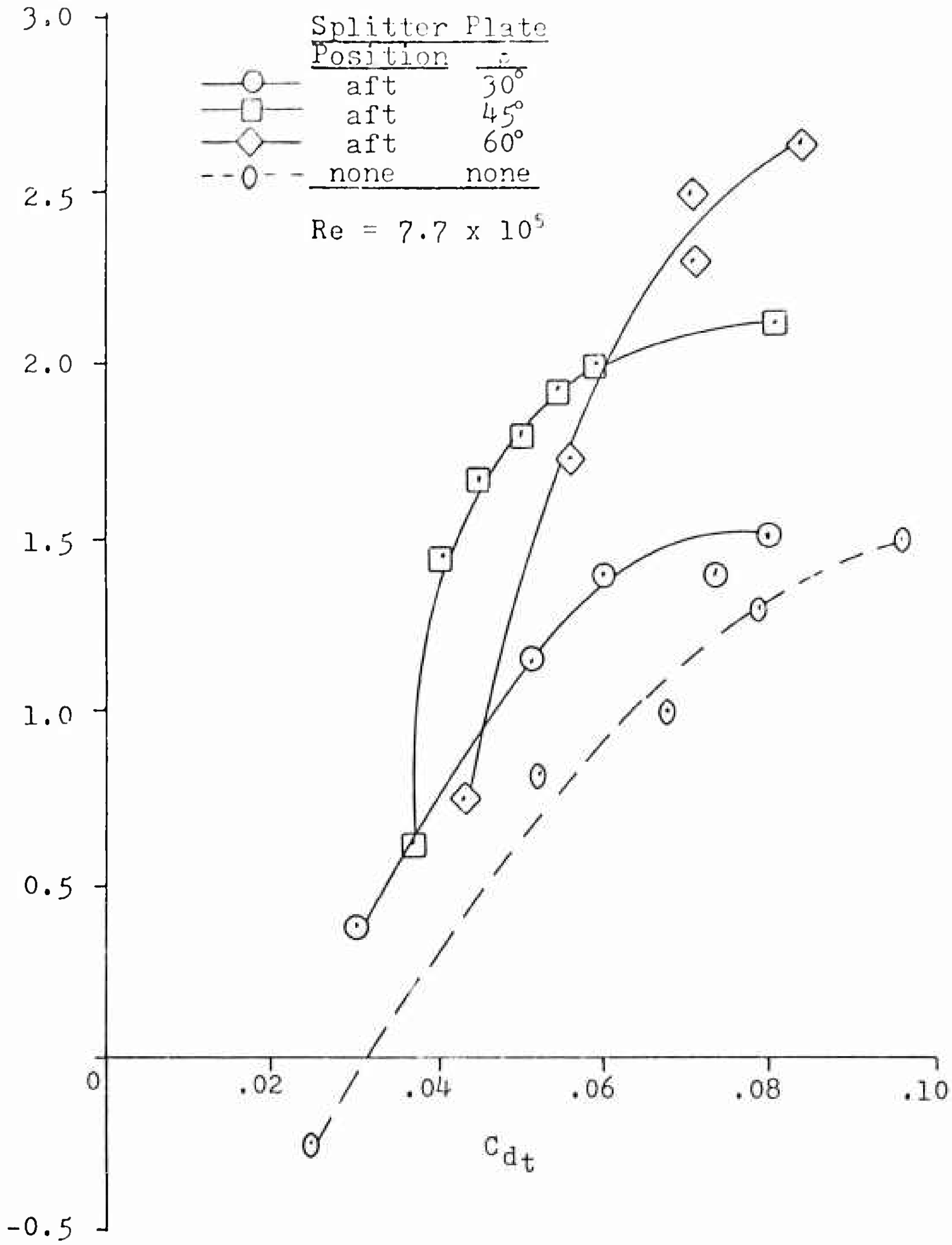

Fig. 27. C_ℓ vs C_{d_t} For Four Airfoil Splitter Plate Configurations at an α_g of -6 Degrees and Increasing C_μ

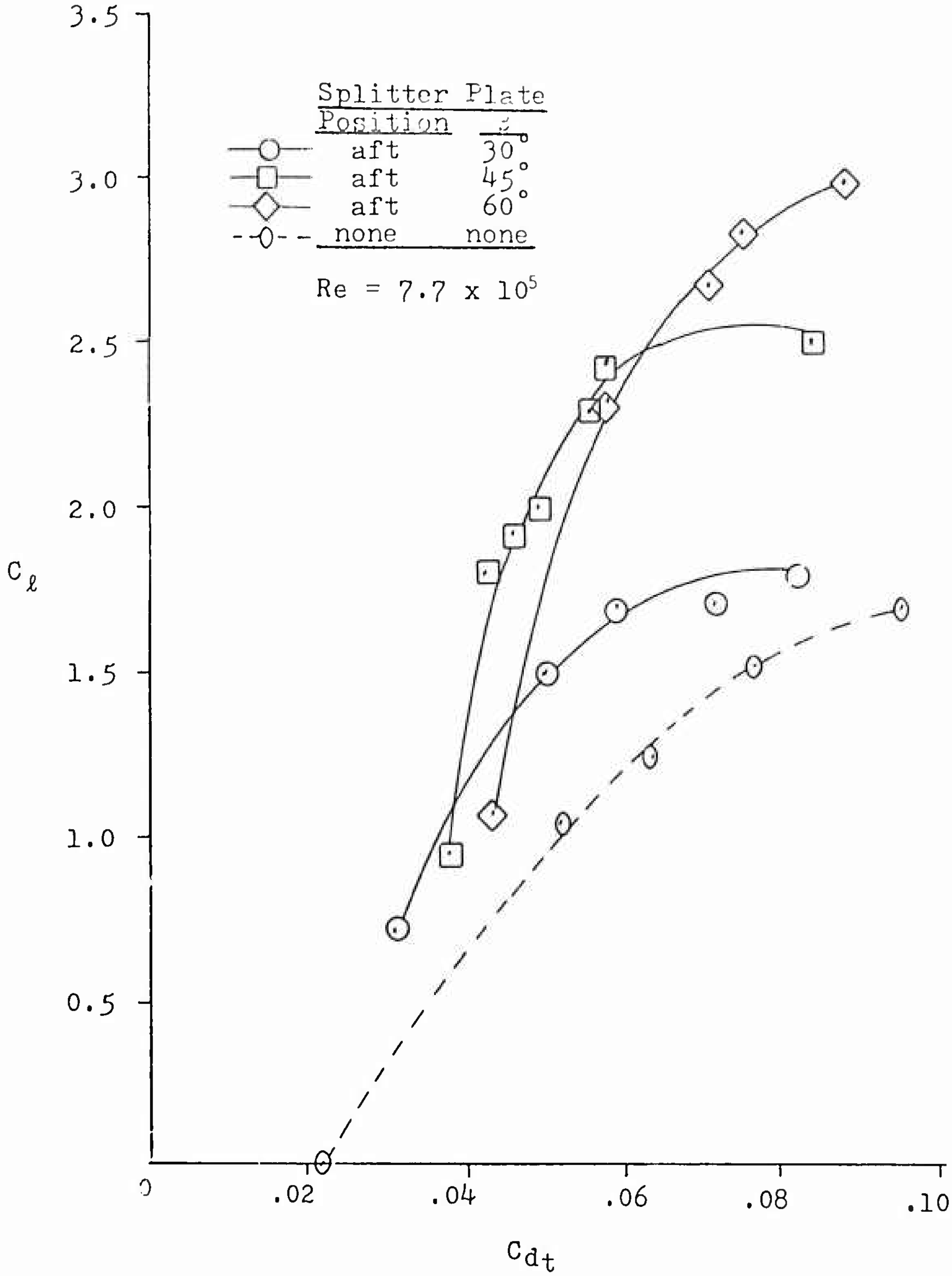

Fig. 28. C_ℓ vs C_{d_t} For Four Airfoil Splitter Plate Configurations at an α_g of -4 Degrees and Increasing C_μ

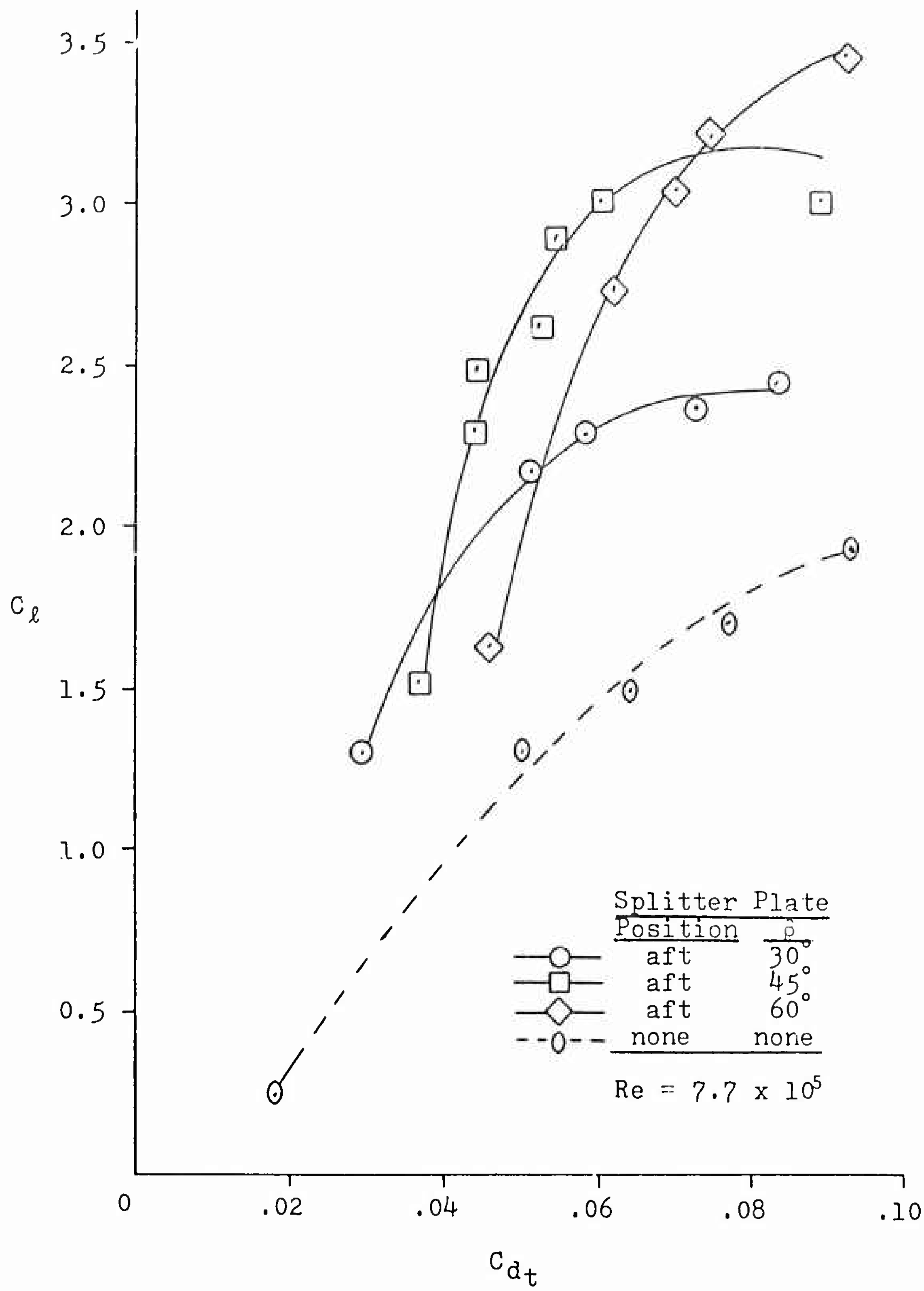

Fig. 29. C_ℓ vs C_{d_t} For Four Airfoil Splitter Plate Configurations at an α_g of -2 Degrees and Increasing C_μ

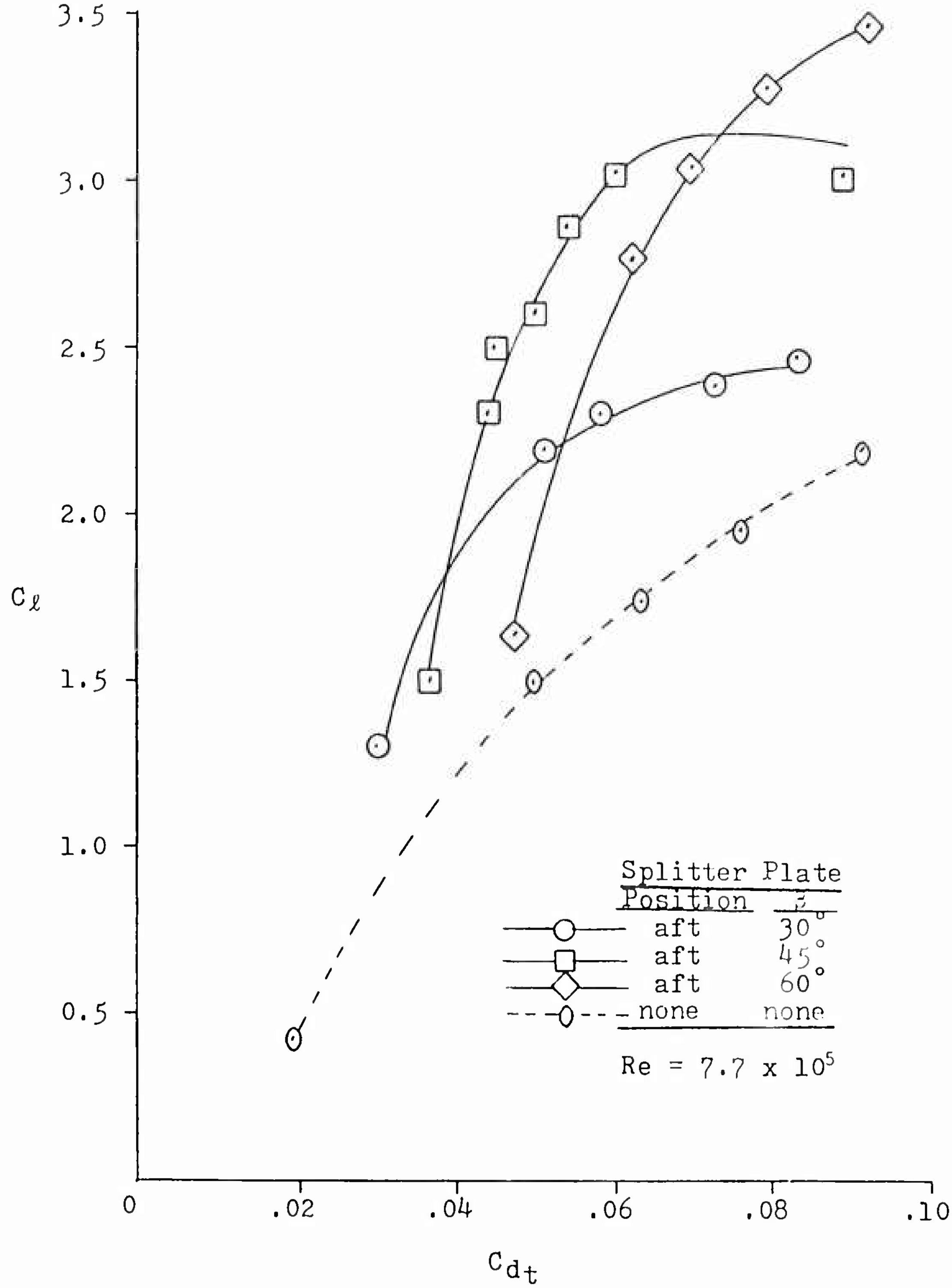

Fig. 30. C_ℓ vs C_{d_t} For Four Airfoil Splitter Plate Configurations at an α_g of 0 Degrees and Increasing C_μ

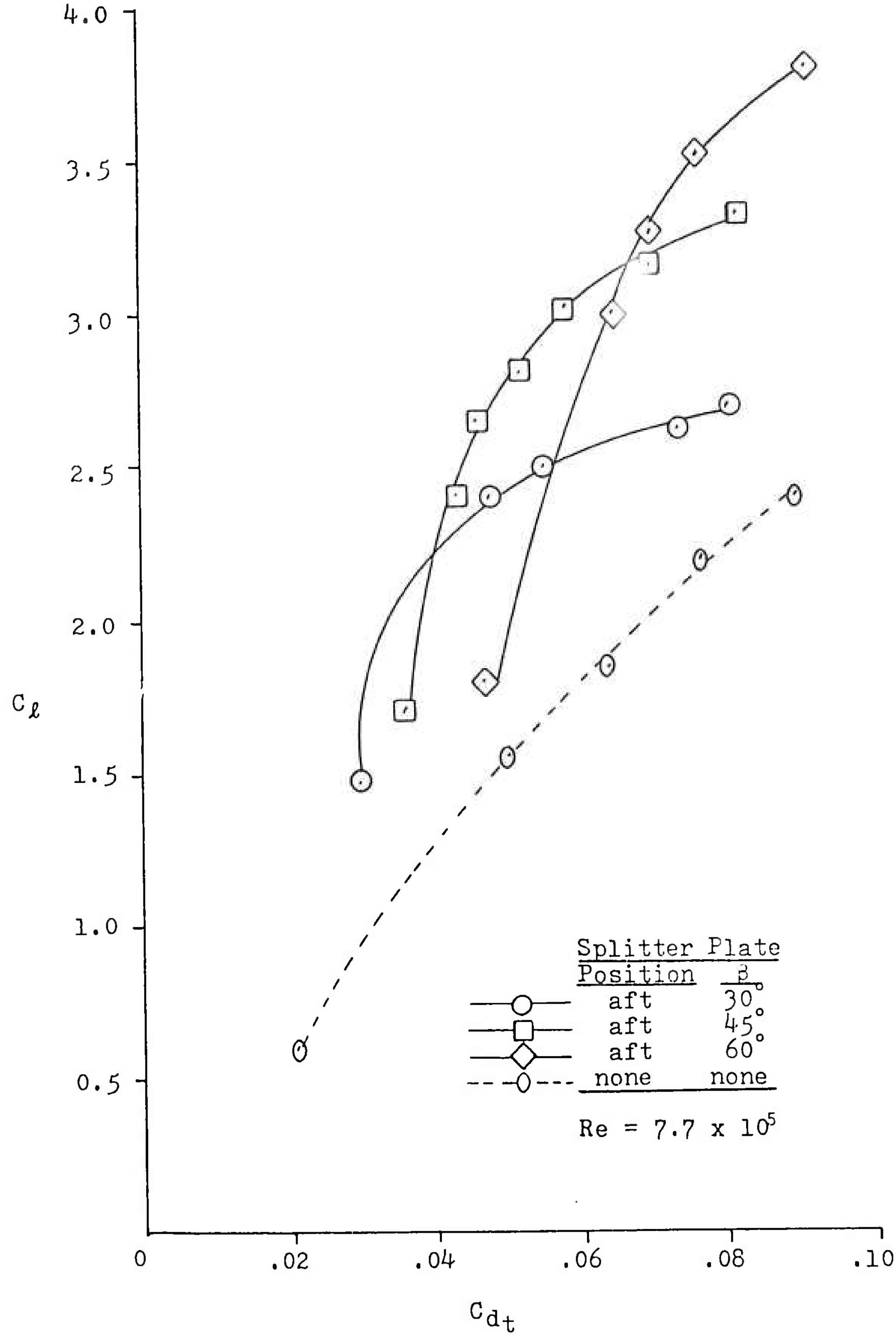

Fig. 31. C_ℓ vs C_{d_t} For Four Airfoil Splitter Plate Configurations at an α_g of +2 Degrees and Increasing C_μ

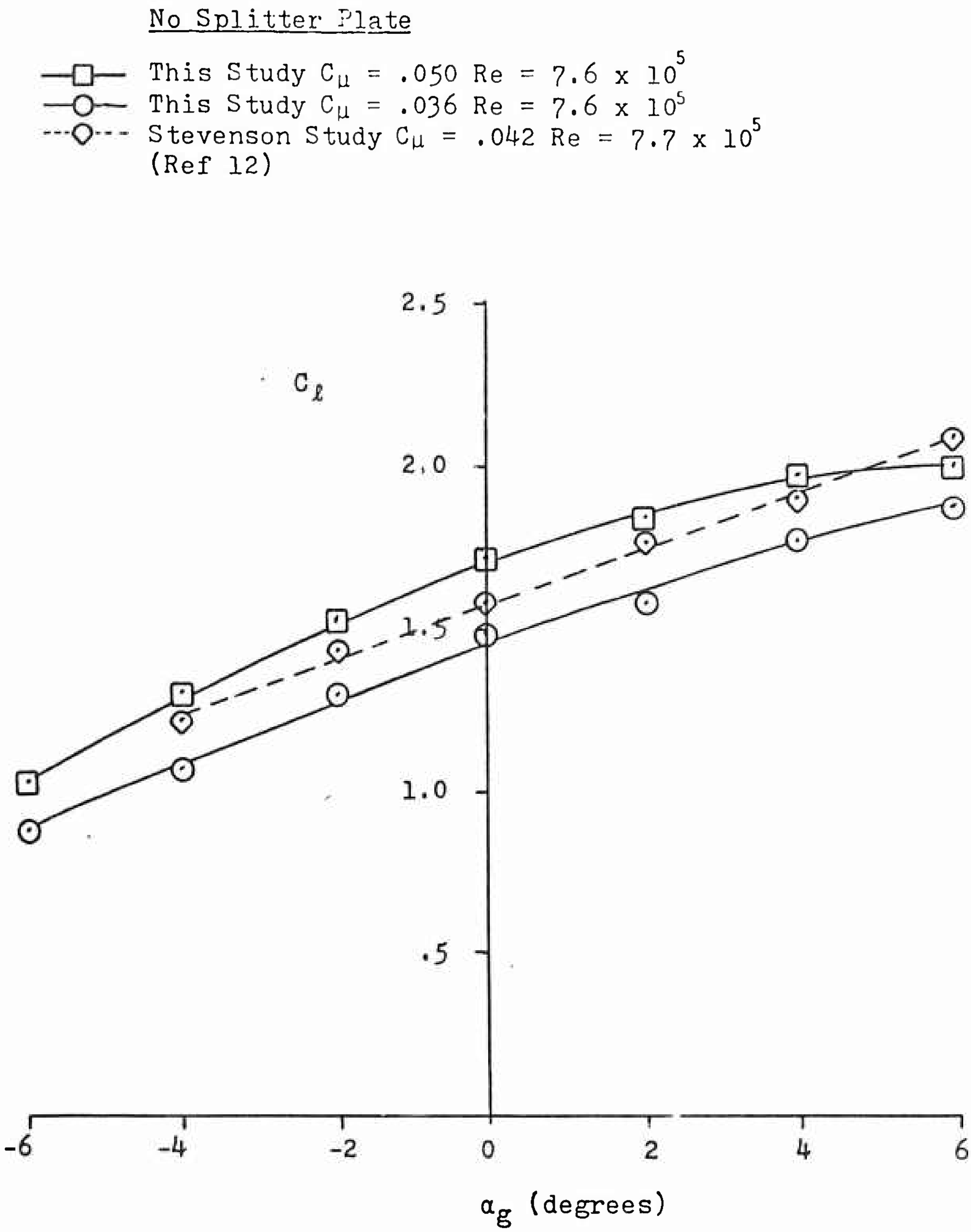

Fig. 32. C_ℓ vs α_g For Two Wind Tunnel Studies

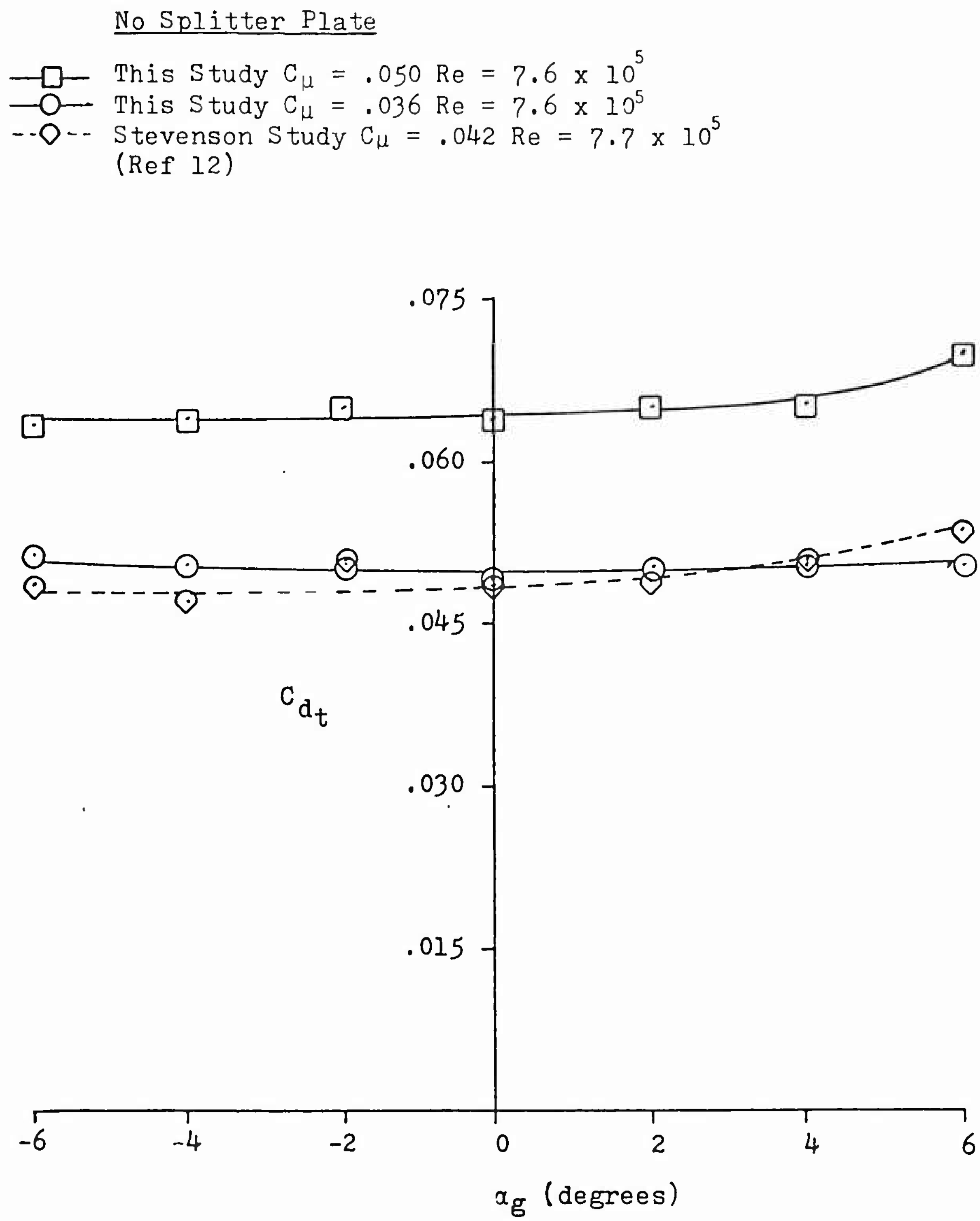

Fig. 33. C_{d_t} vs α_g For Two Wind Tunnel Studies

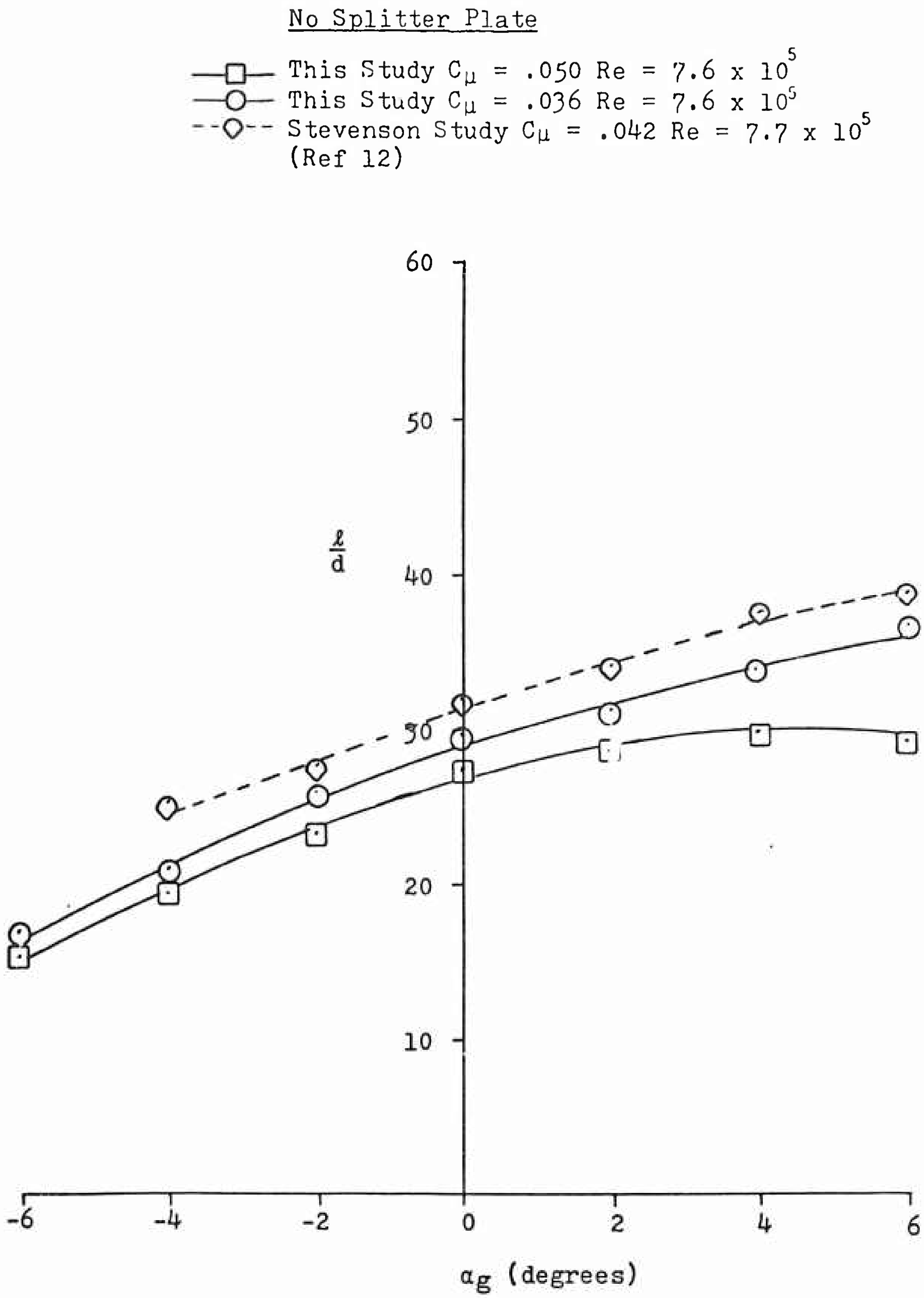

Fig. 34. ℓ/d vs α_g For Two Wind Tunnel Studies

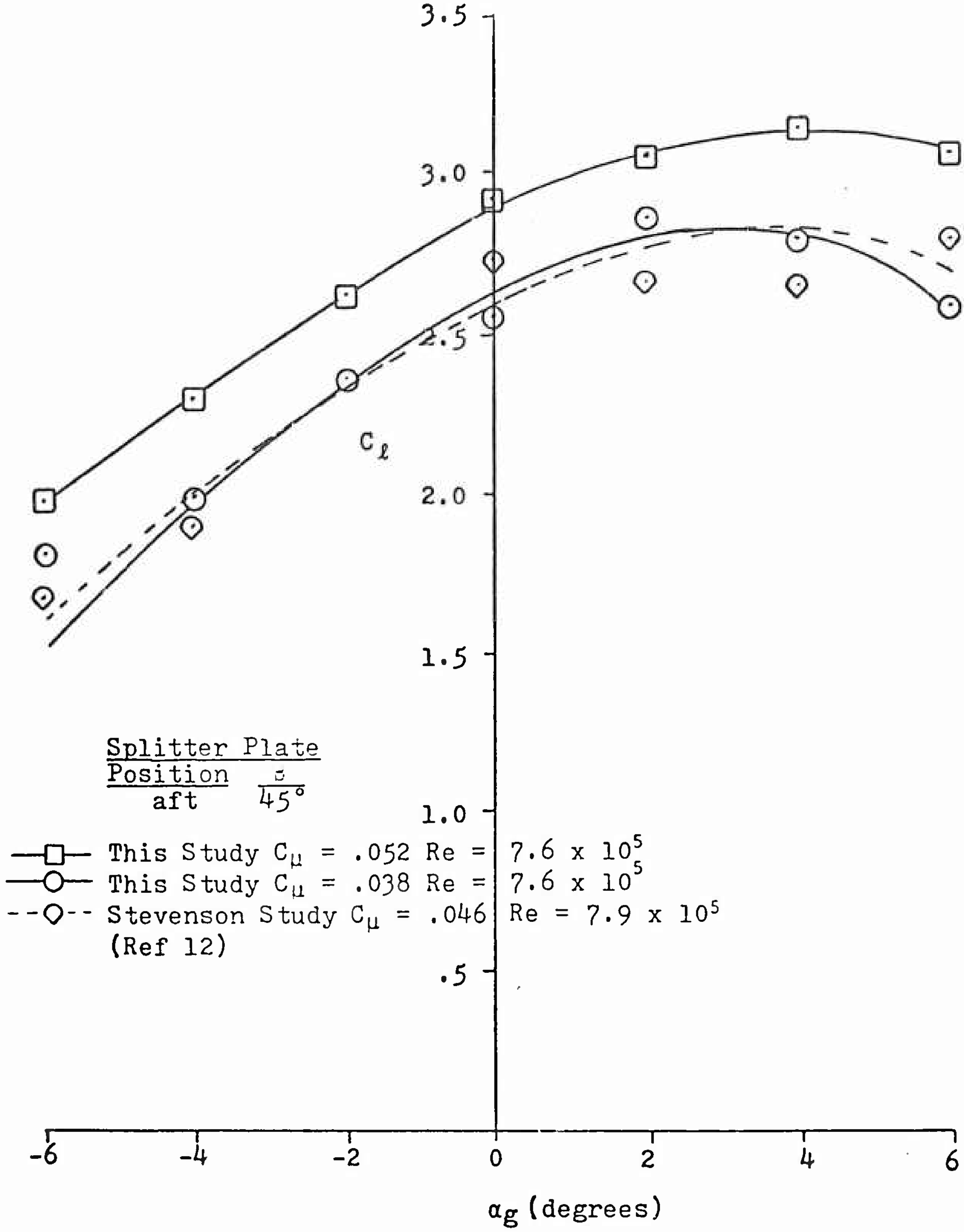

Fig. 35. C_ℓ vs α_g For Two Wind Tunnel Studies

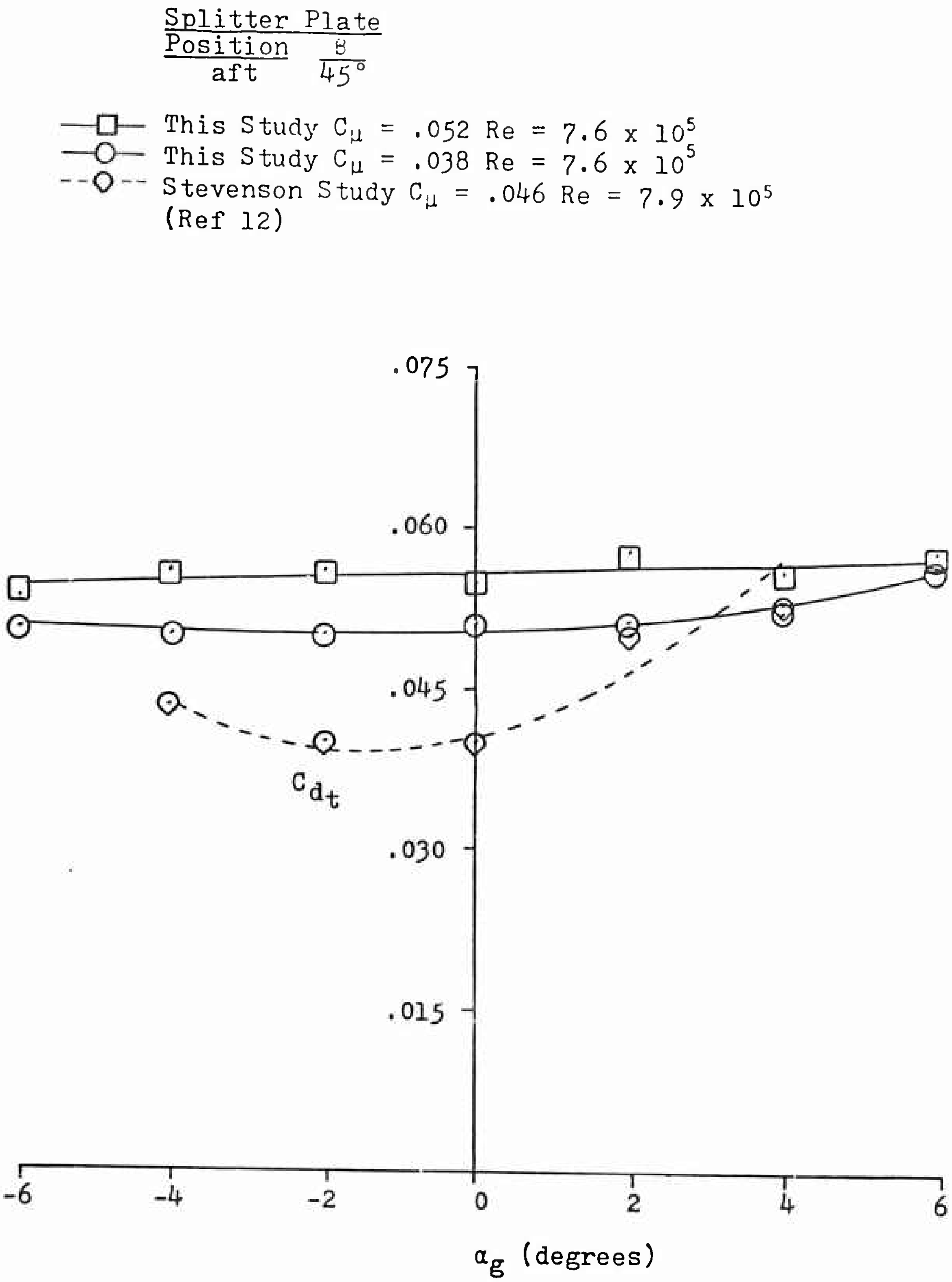

Fig. 36. C_{d_t} vs α_g For Two Wind Tunnel Studies

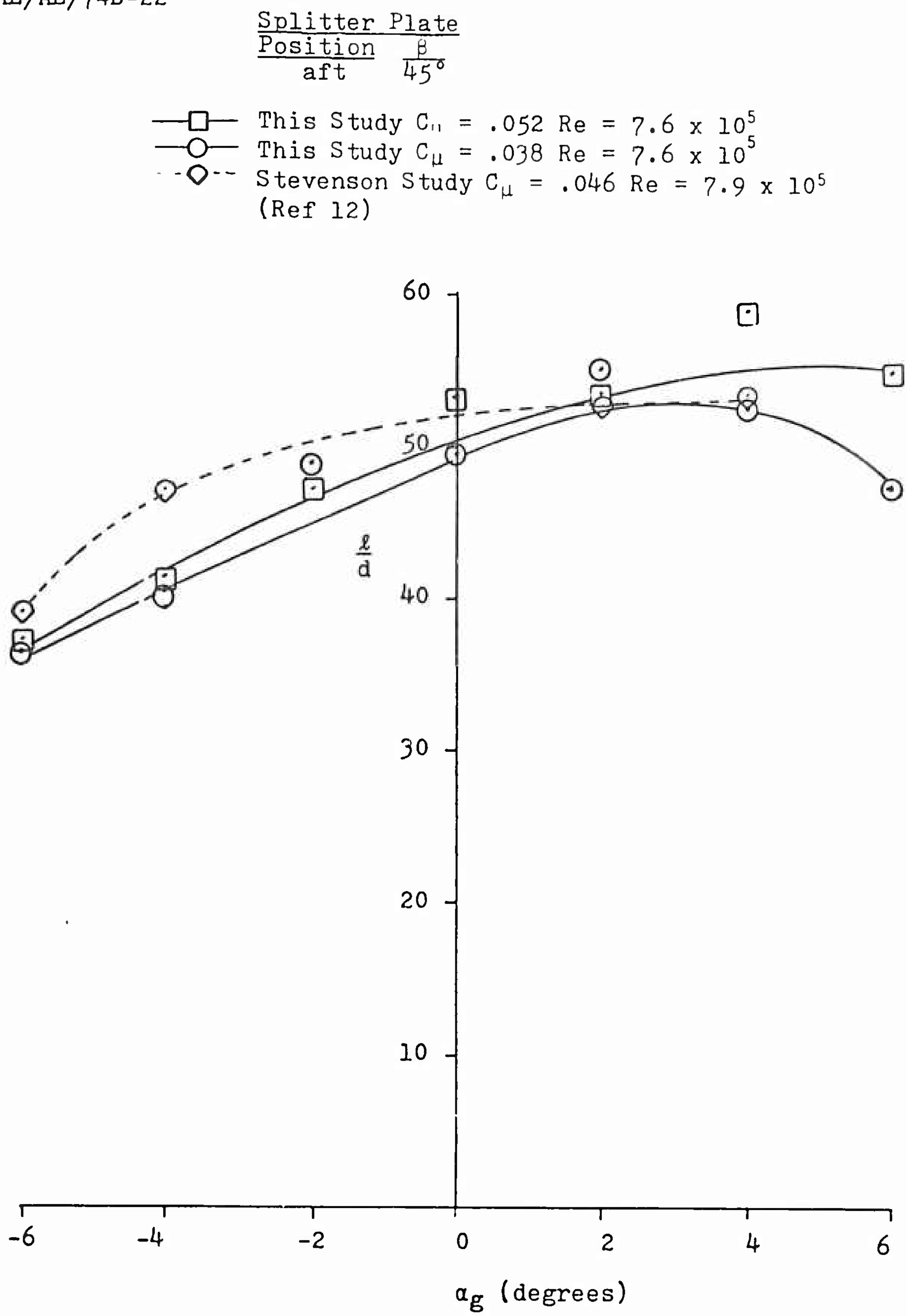

Fig. 37. ℓ/d vs α_g For Two Wind Tunnel Studies

Vita

Wayne Edgar Rhynard Jr. was born [redacted] He graduated from [redacted] in 1962, and attended the United States Air Force Academy, receiving a Bachelor of Science degree and a commission in the United States Air Force in June 1966. Following graduation from pilot training he served as an F-4 pilot at George Air Force Base, California, for 28 months in Southeast Asia, and at Holloman Air Force Base, New Mexico. He began study at the Air Force Institute of Technology in June 1973.

Permanent address: [redacted]

This thesis was typed by Miss Linda K. Moenter.